Calculating the Impedance Profile of the AC Network at a HVDC Link via Modulation of the Inverter's Firing Angle Signal

By

Robin Sue Smyrski

A Thesis

Submitted to the Faculty of Graduate Studies in partial fulfillment of the requirements for the degree of

Master of Science

The Department of Electrical and Computer Engineering

The University of Manitoba
Winnipeg, Manitoba, Canada

THE UNIVERSITY OF MANITOBA

FACULTY OF GRADUATE STUDIES

*****

COPYRIGHT PERMISSION

Calculating the Impedance Profile of the AC Network at a HVDC Link via Modulation of the Inverter's Firing Angle Signal

by

Robin Sue Smyrski

A Thesis/Practicum submitted to the Faculty of Graduate Studies of The University of Manitoba in partial fulfillment of the requirement of the degree

of

Master of Science

Abstract

Knowledge of the characteristics of the AC network impedance at a high voltage direct current (HVDC) link is of vital importance to the operation of the link. The purpose of this thesis was to develop a method to accurately determine the AC network impedance characteristics at a HVDC link. Impedance profiling was achieved by measuring the current entering the AC network and the voltage of the AC bus bar while modulating the HVDC inverter's firing angle signal. Specific impedance profiling techniques were tested using various network impedances and DC current orders. In addition, the ride-through capability of a HVDC link with a modulated firing angle was examined.

The AC network impedance at a HVDC link can be quickly identified over a wide frequency band via multiple frequency modulation of the converter's firing angle signal. The optimum time for impedance profiling is when the DC current order is set at a low value. Impedance profiling should not be attempted during a significant system transient as the accuracy of the calculated impedance profile may be compromised. The phase of each frequency component in the modulation signal should be staggered to avoid disturbing system operation. Also, the number of modulation frequencies should be limited to avoid large interactions between the HVDC control system and modulation signal. As the AC network strength increases, the magnitude of each frequency component in the modulation signal must be increased to guarantee measurable harmonic voltages are generated at the AC bus bar. A Discrete Fourier Transform technique with

high sampling frequency should be used to calculate the harmonic components in the measured AC signals.

A HVDC link with a modulated firing angle has ride-through capability. Firing angle modulation does not negatively affect system performance following an AC single line to ground fault, a DC line fault or a change in DC current order.

The impedance profiling method developed in this thesis can be used in future system optimization studies. Network resonances could be resolved and impedance dependent operating procedures and protection, damping and control systems could be developed. In addition, the research completed in this thesis supports future studies of the feasibility of modulating the control signals of various flexible AC transmission systems.

The software models created for this thesis use Power System Computer Aided Design/Electromagnetic Transients Direct Current software. Future work can be completed to convert these models to equivalent software models on the Real Time Digital Simulator (RTDS), producing simulations in real time. The developed impedance profiling method could be physically implemented in an impedance monitor hardware device which could be tested using RTDS software and then used in an operating power system.

Acknowledgements

I am grateful to the many people whose time and effort have contributed to the completion of this thesis.

First, I would like to thank Dr. A.M. Gole (Department of Electrical and Computer Engineering, University of Manitoba), my academic advisor, for his helpful insights, knowledge, guidance and patience throughout the project. His expertise in HVDC systems and AC/DC conversion has been invaluable. His lively and energetic personality has made this an enjoyable learning experience.

In addition, I want to thank Tony Weekes (System Performance, Manitoba Hydro). His vision and enthusiasm for this thesis pointed me in the right direction and his knowledge of AC/DC systems and communication theory helped me in my technical analysis.

I am extremely grateful to David Jacobson (System Planning, Manitoba Hydro) for his innovative ideas and for generously allowing me to spend some time at work on this thesis these past two years.

Table of Contents

List of Figures

List of Figures (continued)

List of Figures (continued)

List of Figures (continued)

List of Figures (continued)

List of Symbols

V_{bb} : rated inverter AC bus bar voltage (root mean square (RMS), line-line quantity)

$Z_{network}$: inverter AC network impedance vector at the fundamental frequency of the AC system

P_{dc} : rated DC power of the HVDC link

$Z_{filters}$: impedance vector corresponding to the overall impedance of the inverter AC filters at the fundamental frequency of the AC system

R: resistor

L: inductor

C: capacitor

f: frequency

f_o: fundamental frequency

υ : frequency of the single frequency modulation signal

X: Discrete Fourier Transform of x

T: sampling period

t_s: sampling instant

N: number of sampling instances per fundamental period

n: harmonic number

Tn: period of the n^{th} harmonic

Y_a: phase a voltage or current vector at a specific frequency

Y_b: phase b voltage or current vector at a specific frequency

Y_c: phase c voltage or current vector at a specific frequency

Y_{a1}: positive sequence component of Y_a

Y_{b1}: positive sequence component of Y_b

Y_{c1}: positive sequence component of Y_c

Y_{a2}: negative sequence component of Y_a

Y_{b2}: negative sequence component of Y_b

Y_{c2}: negative sequence component of Y_c

γ : extinction angle

γ_{min} : inverter minimum extinction angle

t_{off}: turn-off time of the inverter thyristor valves

$\Delta\alpha$: firing angle modulation signal

t: time

m: phase staggering exponent

k_υ : magnitude of the single frequency modulation signal

ϕ_υ : phase of the single frequency modulation signal

α : firing angle control signal after the addition of the modulation signal

α_{cs} : firing angle control signal prior to the addition of the modulation signal

V_{dc} : DC voltage

V_l : fundamental inverter AC bus bar voltage referred to the secondary side of the inverter transformers (RMS, line-line quantity)

List of Symbols (continued)

X_c : commutating reactance of the inverter transformers

I_{dc} : DC current

μ : overlap angle

Index Terms

1) Calculating the Impedance Profile of the AC Network at a HVDC Link
2) Modulating the Firing Angle Signal of a HVDC Inverter
3) Comparing the Fourier Transform Analysis Techniques used in Impedance Profiling
4) Investigating the Impact of a HVDC Control System on Impedance Profiling
5) Testing the Accuracy of the Impedance Profile for Various Network Impedances and Loading Conditions
6) Verifying the Ride-through Capability of a HVDC Link with a Modulated Firing Angle

Chapter 1: Introduction

The purpose of this thesis is to develop a method to accurately determine the AC network impedance characteristics at a HVDC link.

Previous work has been completed in this area. One approach to impedance identification is to inject currents of varying frequencies into the network and calculate the impedance from current and voltage measurements [1, 2, 3]. This approach has been tested via computer simulations with the network modeled in detail. To implement this method on an actual power system, the impedance of interest must be disconnected from the power system during current injection. This is a major disadvantage of the current injection approach. Other impedance measurement approaches have involved measuring the non-fundamental frequency signals generated by natural disturbances or induced transients [4, 5]. Disadvantages to these approaches include a low signal to noise ratio (SNR) during measurement and difficulty generating low order harmonic frequencies.

This thesis investigates the feasibility of AC network impedance measurement via modulation of the HVDC inverter's firing angle signal. The goal is to create a modulation signal that can be used to determine the AC network impedance profile over a frequency range without disturbing system operation. Modulation and impedance

measurement would occur while the AC network impedance is connected to the operating power system.

Previous research has been conducted investigating the possibility of using firing angle modulation to determine the AC network impedance profile [6]. The previously proposed impedance monitor encountered difficulties in determining the impedance phase. Also, the impedance magnitude could not be accurately identified at frequencies higher than three times the fundamental frequency.

The Power System Computer Aided Design/Electromagnetic Transients Direct Current (PSCAD/EMTDC) computer software program was used to complete the research for this thesis. When the AC network impedance is modeled using linear components, one can calculate the impedance profile using phasor analysis. However, when the AC network contains nonlinear components, the benefit of PSCAD/EMTDC becomes apparent. The fundamental frequency impedance of a nonlinear AC network can be measured at various operating points through PSCAD/EMTDC simulations at the operating points of interest. When the AC network contains controlled equipment, the control responses are included in the PSCAD/EMTDC impedance measurement.

1.1 AC Network Impedance Characteristics at a HVDC Link

In the era of power system deregulation and competitive power markets, the real-time impedance profile of the AC network has the potential to be quite different from the forecasted or predicted impedance profile.

Knowledge of the characteristics of the AC network impedance at a HVDC link is of vital importance to the operation of the HVDC link. The fundamental frequency impedance of the AC network affects the commutating voltage of the HVDC link [7]. Commutating voltage refers to the AC bus bar voltage responsible for transferring current from the off-going thyristor valve to the on-going thyristor valve. When the fundamental frequency impedance is small, the AC system is considered strong and the commutating voltage does not vary greatly. In contrast, when the fundamental frequency impedance is large, the AC system is considered weak and the commutating voltage may experience large variations.

The strength of the AC system can be quantified by calculating the Short Circuit Ratio (SCR) and Effective Short Circuit Ratio (ESCR) of the system. The inverter AC system SCR is defined as

$$SCR = \frac{V_{bb}^{\ 2}}{Z_{network}^{\ *} * P_{dc}}$$

where: V_{bb} is the rated inverter AC bus bar voltage (RMS, line-line quantity)

$Z_{network}$ is the inverter AC network impedance vector at the fundamental frequency of the AC system

P_{dc} is the rated DC power of the HVDC link [8]

The inverter AC system ESCR is defined as

$$ESCR = \frac{V_{bb}^{\ 2}}{(Z_{network} \,//\, Z_{filters})^{*} * P_{dc}}$$

where: $Z_{filters}$ is impedance vector corresponding to the overall impedance of the inverter AC filters at the fundamental frequency of the AC system [8]

An AC system is considered strong when it has an ESCR greater than 2.5. It is considered very strong when it has an ESCR greater than 5. A weak AC system has an ESCR less than 2.5 and a very weak system has an ESCR less than 1.5.

It is common for the commutating voltage in weak AC systems to undergo large fluctuations. These large voltage variations can prevent the normal transfer of current flow between converter thyristor valves. A lack of current transfer between valves is known as commutation failure [7]. As the AC system becomes weaker, the risk of commutation failure increases.

It is important to accurately identify harmonic resonances in the AC network impedance. Harmonic instability can occur when the DC system has a resonant impedance that complements an AC network harmonic resonance [8, 9]. Stability problems arise when voltage harmonics develop on the AC system at the harmonic resonant frequency of the AC network. An especially worrisome resonance is a second harmonic AC network resonance. Second harmonic currents and voltages are often seen on AC systems, as they

are generated during transformer saturation. When the DC system has a complementary resonance the HVDC converter can magnify the harmonic AC voltage. When this harmonic magnification is extreme the converter is said to exhibit harmonic instability. The harmonic voltages and currents produced in the AC and DC systems can become excessive. This is catastrophic for the operation of a HVDC link.

An operating HVDC converter produces AC harmonic currents. The harmonic currents that are produced during normal converter operation are called characteristic harmonics [8]. The converter AC filters are designed to prevent characteristic harmonics from propagating through the AC network. However, actual AC filters do not always perform ideally and so some characteristics harmonics may enter the AC network. System stability problems can arise when the AC network has a harmonic resonance at a characteristic harmonic. The characteristic harmonic current can produce a large harmonic voltage on the AC system. Power system performance is degraded when a large AC harmonic voltage develops.

Knowledge of the AC network impedance profile allows for verification and enhancement of existing models of the network. In addition, network harmonic resonances could be resolved and system performance could be optimized. One could implement protection, damping and control systems that are dependent on the existing network impedance profile [10]. For example, damping system gains could respond in real time to the changing network impedance.

1.2 Main Focus of Thesis

The main focus of this thesis is the investigation of a technique to accurately determine the AC network impedance characteristics at a HVDC link. The impedance characteristics are calculated by measuring the current entering the AC network and the voltage of the AC bus bar while modulating the HVDC inverter's firing angle signal.

A small modulation signal is required to ensure system operation is not disturbed. However, the modulation signal must be large enough to generate measurable voltages and currents. This thesis investigates many possible modulation signals. Both single and multiple frequency sinusoidal injections are considered.

Two methods are used in calculating the impedance profiles – a Fast Fourier Transform (FFT) method with a low sampling frequency and a Discrete Fourier Transform (DFT) method with a high sampling frequency [11]. Comparisons between the two methods are made to determine the optimal calculation method. The FFT method is typically what is used in computerized protection relay models and uses a relatively small sampling rate so as to keep in step with "real time". This constraint is not present in offline data processing. When using the DFT method, data is processed offline. Hence, the results from the DFT method are expected to be more accurate.

With the FFT method, immediate impedance identification is achieved by constantly sampling the filtered AC bus bar voltage and current entering the AC network. In order to obtain the correct spectrum, these voltage and current signals are passed through anti-

aliasing filters to eliminate the higher frequency components in the signals. The signals are then sampled at twice the highest remaining frequency component in the signals, in accordance with Shannon's sampling theorem [11]. FFT analysis is conducted continuously while harmonics are being generated on the operating AC system. With continuous FFT analysis, there is loss of continuity of information. At each sampling instant a new set of sampled data is used and the previous set of data is discarded.

With the DFT method, impedance identification is achieved by sampling the AC bus bar voltage and current entering the AC network for a period of time while harmonics are being generated on the operating AC system. DFT analysis is used to decompose the voltage and current into their frequency components. This decomposition requires a finite amount of time. When doing DFT analysis, the voltage and current were sampled at an extremely high rate.

Both the DFT and the FFT have inherent sources of error, as they are approximations of the discrete-time Fourier Transform [11]. Reducing the sampled data to zero outside of the time frame under consideration causes some error. This abrupt truncation of the sampled data results in a calculated frequency spectrum that is spread across a larger range of frequencies than the actual frequency spectrum of the sampled signal. This is known as spectrum-leakage distortion [11]. Spectrum-leakage distortion can be reduced by multiplying the sampled data by a function that peaks at a value of one during the time frame under consideration and gradually approaches zeros at the limits of the time frame under consideration. Two functions that are commonly used are the Hamming window

and the Hanning window [11]. The research completed in this thesis does not investigate the reduction of spectrum-leakage distortion.

The accuracy of the impedance profiling methods is tested for various network impedances and DC current orders. Using a simplified model of a HVDC link, impedance profiles are generated for resistive-inductive (RL), RRL, RLL and resistive-resistive-inductive-inductive-capacitive-capacitive (RRLLC) type impedances. This simplified model includes a detailed model of the HVDC inverter with the rectifier modeled as a DC voltage source. The HVDC controls are not modeled – instead a constant firing angle control signal is assumed. Using a HVDC link benchmark model proposed by the International Council on Large Electric Systems (CIGRE) [12], impedance profiles are generated for weak and strong AC networks. Impedance profiles are also taken at DC current orders of 1 P.U., 0.7 P.U. and 0.5 P.U. This benchmark model contains detailed modeling of the HVDC rectifier, inverter and control system.

The impact of a HVDC control system on impedance profiling is also investigated using the CIGRE benchmark model. A low interaction between the control system and the modulation signal is desired.

In addition, the ride-through capability of a HVDC link with a modulated firing angle is verified using the CIGRE benchmark model. Many system transients and disturbances are considered. These include a 10% increase or decrease in DC current order, an AC single line to ground (SLG) fault at the inverter and a DC line fault.

Results of the investigations show a single frequency modulation signal can easily be used to modulate the firing angle, have negligible effect on system operation and obtain an impedance profile at specific frequencies. When using multiple frequency modulation signals, care must be taken to ensure the system operation is not appreciably affected.

The DFT method with high sampling frequency appears superior to the FFT method with low sampling frequency. The FFT method was often inaccurate at frequencies around five and a half times the fundamental frequency and at frequencies higher than seven and a half times the fundamental frequency. Inaccuracies were sometimes evident at other frequencies. The DFT method is often quite accurate in impedance profiling. Accurate impedance calculations were obtained at frequencies ranging from 5 Hz to eight times the fundamental frequency.

The RL, RRL, RLL and RRLLC impedance types can all be accurately profiled. In addition, impedance measurement is possible over a range of system conditions and operating points. In general, decreasing the DC current order improves the accuracy of the calculated impedance profile. When the system has a strong AC network, the magnitude of the modulation often must be increased to obtain measurable harmonic voltages at the AC bus bar. When the system has a weak AC network, the modulation magnitude often must be decreased to avoid affecting system operation.

The HVDC control system does interact with the modulation signal and does affect the impedance measurements. To limit the interaction, the multiple frequency modulation signal should have a limited frequency range.

A HVDC link with a modulated firing angle has ride-through capability for a change in DC current order, an AC SLG fault and a DC line fault.

The research work completed can be extended in future studies. Rapid identification of the AC network impedance at a HVDC link could be used to optimize system performance. Network resonances could be resolved and impedance dependent operating procedures and protection, damping and control systems could be developed.

Modulation of the control signals of various power electronic devices and flexible AC transmission systems (FACTS) could be investigated. For example, one could modulate the thyristor controlled reactor (TCR) control signal of a static VAr compensator (SVC) in an attempt to measure the impedance at that specific point in the power system. In addition, the SVC protection, damping and control systems could be made impedance dependent to enhance system reliability, stability and security.

The research models created for this thesis use PSCAD/EMTDC software. Future work could be completed to convert these models to equivalent software models on the Real Time Digital Simulator (RTDS), producing simulations in real time.

A physical prototype of an impedance monitor could be built. This hardware device would use the techniques investigated in this thesis to monitor the AC network impedance at a HVDC link via modulation of a HVDC converter firing angle. The prototype could be wire wrapped or a breadboard could be used. The impedance monitor prototype could be tested using RTDS software.

Ultimately, an impedance monitor could be built for use in an operating power system. This would involve card design with solder masked and would be completed after the impedance monitor prototype was tested using RTDS software.

1.3 Overview of Thesis

The thesis is divided into six chapters. The introductory chapter provides an overview of the thesis and discusses the purpose, scope and findings of the thesis.

Chapter 2 presents various approaches to AC network impedance identification at a HVDC link. One approach is to inject current of varying frequencies into the AC network impedance. Another method is to modulate the firing angle of the converter with a specified modulation signal. There are a variety of ways in which the impedance profile can be calculated from measured system data. The two methods discussed in Chapter 2 are a Fast Fourier Transform method and a Discrete Fourier Transform method.

The research completed for this thesis focuses on the feasibility of AC network impedance measurement via modulation of the HVDC inverter firing angle signal. Chapter 3 discusses the approach taken in the research work and outlines the theory behind impedance profiling via firing angle modulation.

Simulation results are presented in Chapters 4 and 5. Chapter 4 shows the impedance profiles calculated for various AC network impedance types and also displays calculated impedance profiles taken at varying network strengths and DC current order settings. Chapter 5 discusses simulations conducted to verify the ride-through capability of a HVDC link with a modulated firing angle. Changes in DC current order and AC and DC line faults are considered.

Conclusions and recommendations for future work are made in Chapter 6.

Chapter 2: Approaches to AC Network Impedance Identification at a HVDC Link

There are various approaches to AC network impedance identification at a HVDC link. One method involves injecting current of varying frequencies into the AC network impedance. Another method requires modulation of the firing angle of the converter with a specified modulation signal.

There are a variety of ways in which the impedance profile can be calculated from measured system data. Two methods will be discussed – a Fast Fourier Transform (FFT) method with low sampling frequency and a Discrete Fourier Transform (DFT) method with high sampling frequency. Using the FFT method, immediate impedance identification is achieved by constantly sampling the filtered AC bus bar voltage and current entering the AC network. FFT analysis is conducted continuously while harmonics are being generated on the operating AC system. Using the DFT method, impedance identification is achieved by sampling the AC bus bar voltage and current entering the AC network for a period of time while harmonics are being generated on the operating AC system. DFT analysis is used to decompose the voltage and current into their frequency components.

2.1 Current Injection

Impedance profiles of electrical devices or subsystems are often obtained through current injection. Injecting sinusoidal currents at a known frequency will produce voltages at known frequencies. In a simple case, injected currents at frequency f will produce voltages at frequency f. This is the case for a resistive-inductive-capacitive (RLC) load. For nonlinear devices, injected currents at frequency f can produce voltages at frequency f as well as sideband voltages at frequencies other than f. For example, injecting a positive sequence current at frequency f into a static synchronous compensator (STATCOM) produces a positive sequence voltage at frequency f and a negative sequence voltage at frequency $(f - 2\ f_o)$, where f_o is the fundamental frequency of the system [3]. Injecting a negative sequence current at frequency f into a STATCOM produces a negative sequence voltage at frequency f and a positive sequence voltage at frequency $(f + 2\ f_o)$.

To determine an impedance profile over a range of frequencies, the injected currents often consist of a summation of sinusoidal currents at multiple frequencies. For linear devices or subsystems, or in cases where the disturbance caused by the injection does not significantly affect the system operating point, superposition is valid and the voltages produced by the injection will be the sum of the voltages produced from each of the sinusoidal current components in the injection signal. When dealing with nonlinear devices, care must be taken to ensure no sideband voltages have the same sequence and frequency as any sinusoidal current component in the injected currents.

The impedance profile of the device or subsystem can be easily calculated by measuring the currents through and voltages across the device or subsystem. First, the currents and voltages are separated into their frequency components. Next, each frequency component is separated into its sequence components. For each frequency and sequence component in the injected current, the corresponding impedance is obtained by taking the ratio of the sequence voltage over the sequence current at that frequency.

As previously mentioned, the major disadvantage in implementing this method is that the device or subsystem to be profiled is often disconnected from the power system during current injection. When profiling an AC network impedance at a HVDC link, the current injection method would involve disconnecting the impedance from the power system, which is not feasible.

2.2 Modulation of the Converter's Firing Angle Signal

One approach to AC network impedance identification at a HVDC link involves modulation of the converter's firing angle signal. The AC network impedance at the HVDC rectifier can be identified via modulation of the rectifier's firing angle signal. Similarly, the AC network impedance at the HVDC inverter can be identified via modulation of the inverter's firing angle signal. The modulation signal is added to the firing angle control signal while the power system is in operation. Careful selection of the modulation signal ensures system operation is not significantly affected while the modulation takes place.

A single frequency sinusoid is a simple choice of modulation signal. As shown in section 3.2, modulating the firing angle signal with a sinusoidal signal of frequency υ will produce harmonic voltages and currents on the AC system. The most significant harmonics will be a positive sequence harmonic at frequency ($\upsilon + f_o$) and a negative sequence harmonic at frequency ($\upsilon - f_o$). Taking the ratio of the AC bus bar voltage over the current entering the AC network impedance at frequency ($\upsilon + f_o$) gives the positive sequence AC network impedance at frequency ($\upsilon + f_o$). Likewise, taking the ratio of the AC bus bar voltage over the current entering the AC network impedance at frequency ($\upsilon - f_o$) gives the negative sequence AC network impedance at frequency ($\upsilon - f_o$). An advantage of single frequency modulation is that the modulation magnitude can be easily chosen to produce AC harmonics that are detectable and measurable without disturbing system operation. However, single frequency modulation is not practical when determining the AC network impedance profile over a wide frequency range, as it involves separately injecting a large number of firing angle modulation signals. Such an undertaking requires many computer simulations and is not practical in terms of time and effort.

At the other extreme, a white noise modulation signal could be added to the firing angle control signal. This would produce AC harmonic voltages and currents over a wide range of frequencies. The AC bus bar voltage and the current entering the AC network could both be monitored and separated into their harmonic frequency and then sequence components. For each harmonic frequency and sequence component, the corresponding impedance could be obtained by taking the ratio of the sequence voltage over the

sequence current at that frequency. In this manner, an AC network impedance profile over a wide frequency range could be quickly generated with one white noise injection. The drawback to white noise modulation is the likelihood of disturbing system operation. When white noise is injected, it is not possible to control the frequency range or magnitude of the AC harmonics that are produced. Although one may be interested in the AC network impedance over a distinct frequency band, the range of produced harmonics on the AC system will likely be much larger than this band making it extremely difficult to detect and accurately measure the current through and voltage across the AC network impedance over the frequency band of interest.

A third option is to choose a multiple frequency sinusoidal signal. When the multiple frequency modulation signal is sufficiently small, it will not cause a significant system disturbance. When the system is not significantly disturbed, it behaves linearly and superposition is valid. It follows that the harmonic voltages and currents produced on the AC system by the modulation signal will be the sum of the harmonic voltages and currents produced from each of the sinusoidal frequency components in the modulation signal. The AC bus bar voltage and the current entering the AC network can both be monitored and separated into their harmonic frequency and then sequence components. For each harmonic frequency and sequence component, the corresponding impedance can be obtained by taking the ratio of the sequence voltage over the sequence current at that frequency.

When the AC network impedance is of interest over a specific frequency band, one can easily determine the frequencies required in a multiple frequency modulation signal. However, a modulation signal that contains all of the required frequencies will not necessarily generate an accurate AC network impedance profile over the entire frequency band of interest. It is evident that each frequency component in the modulation signal must be large enough to generate measurable harmonic voltages and currents. At the same time, the modulation signal must remain small enough to ensure system operation is not disturbed. As discussed in Chapter 3, the magnitude of the modulation signal can be decreased by staggering the phase of each frequency component in the signal. However, even with phase staggering, there is a limit to the number of frequencies that can be included in the modulation signal without disturbing system operation and there are two reasons why the calculated impedance profile will not be accurate when the system operation is disturbed. First, it will be extremely difficult to detect and accurately measure the current through and voltage across the AC network impedance. Second, superposition will not hold and the harmonics produced on the AC system will not cover the expected frequency range. At some frequencies within the range, no harmonic voltages or currents will be produced. Therefore, it may in fact be necessary to inject many separate modulation signals to generate an accurate AC network impedance profile over the frequency band of interest. Notwithstanding this, the advantage of multiple frequency modulation should not be dismissed. Using this type of modulation signal, it is possible to generate an accurate impedance profile over a specific frequency band and this accurate impedance profile can be generated many times faster than could be accomplished using single frequency modulation.

2.3 Calculating the Impedance Profile from Measured System Data

Having generated harmonics on the operating AC system, either via current injection or modulation of the converter's firing angle signal or through another means, the measured AC bus bar voltage and measured current entering the AC network can be analyzed to determine the AC network impedance profile.

When determining an AC impedance profile, all useful information is contained in the harmonic components present in the AC signals. However, as previously discussed, the power system operating point should not be significantly affected while AC system harmonics are generated meaning the generated harmonics should be relatively small in magnitude when compared with the fundamental frequency AC signals. The dominant fundamental frequency components can easily override and detract from the useful harmonic components present in the AC signals. To increase the accuracy of the calculated impedance profile, the fundamental frequency components present in the AC bus bar voltage and current entering the AC network can be removed prior to harmonic analysis of these signals. This can be accomplished using a second order notch reject filter with a characteristic frequency set to the fundamental frequency of the power system. This will also improve the signal to noise ratio (SNR) of the measured AC signals. The SNR of a signal is defined as the power of the useful components over the average power of the useless or noisy components in the signal [13].

When considering impedance profiling over a specific frequency range, all useful information is contained in the AC signal harmonic components that lie within that frequency range. In this case, the SNR of the measured AC signals can be improved by effectively eliminating all frequency components outside the frequency range of interest, as well as the fundamental frequency components, that are present in the AC bus bar voltage and current entering the AC network. This can be accomplished using three second order filters – a high pass filter with a characteristic frequency set slightly lower than the frequency range, a low pass filter with a characteristic frequency set slightly higher than the frequency range and a notch reject filter with a characteristic frequency set to the fundamental frequency of the power system.

To calculate the AC network impedance profile, the filtered three phase AC bus bar voltage and filtered three phase current entering the AC network can be sampled and next decomposed into their harmonic and then sequence components. Before sampling the signals, a low pass anti-aliasing filter can be used to avoid overlap in the sampled signals frequency spectrum, an undesirable side effect inherent in sampling [11]. Discrete Fourier Transform (DFT) analysis or Fast Fourier Transform (FFT) analysis can be used to calculate the harmonic components in the voltages and currents [11]. The FFT is a collection of efficient algorithms that can be used to quickly calculate the DFT. Fourier Transform analysis gives the magnitude and angle of the input signal at the signals fundamental frequency and at a chosen number of harmonics of that fundamental frequency.

The Discrete Fourier Transform is defined as

$$X(\tfrac{2\pi k}{NT}) = T \sum_{t_s=0}^{(N-1)T} x(t_s) * e^{-j2\pi k t_s / TN} \quad \text{for k = 0, 1, 2, ..., N-1}$$

where: $x(t_s)$ is the input signal at sampling instant t_s

$X(\frac{2\pi k}{NT})$ is the Discrete Fourier Transform of the input signal at frequency $\frac{2\pi k}{NT}$

T is the sampling period

N is the number of sampling instances per fundamental period of the input signal

The magnitude of the input signals component at frequency $\frac{2\pi k}{NT}$ is

$$\frac{2}{NT} * | X(\tfrac{2\pi k}{NT}) | \text{ for k = 1, 2, ..., N-1}$$

The angle of the input signals component at frequency $\frac{2\pi k}{NT}$ is

$$\angle X(\tfrac{2\pi k}{NT}) \text{ for k = 0, 1, 2, ..., N-1}$$

When doing Fourier Transform analysis, the sampling rate must be chosen carefully. According to Shannon's sampling theorem, data must be sampled at a minimum rate of $\frac{2}{Tn}$ to calculate the n^{th} harmonic component with period Tn. If data is sampled at a rate lower than this minimum rate, the calculation of the n^{th} harmonic component will be inaccurate [11].

Each of the calculated frequency components in the voltages and currents can be broken down into sequence components using symmetrical component theory [14]. Symmetrical components are often used when writing DC system equations and general power system equations.

As discussed in section 2.2, modulation of the converter's firing angle with a small multiple frequency sinusoidal signal produces harmonic voltages and currents on the AC system that consist of the sum of the harmonic voltages and currents produced from each of the sinusoidal frequency components in the modulation signal. As shown in section 3.2, modulating the firing angle signal with a sinusoidal signal of frequency υ will generate a significant positive sequence harmonic at frequency ($\upsilon + f_o$) and a significant negative sequence harmonic at frequency ($\upsilon - f_o$) on the AC system. Therefore, during multiple frequency modulation of the firing angle, a harmonic voltage or current on the AC system could easily consist of both positive and negative sequence components. Using symmetrical component theory, the positive and negative sequence components of each AC system harmonic can be separated and identified.

The following equations can be used to calculate the sequence components of each of the calculated frequency components in the AC voltages and currents.

$$\begin{bmatrix} Y_{a1} \\ Y_{a2} \end{bmatrix} = \frac{1}{3} * \begin{bmatrix} 1 & 1\angle 120^\circ & 1\angle -120^\circ \\ 1 & 1\angle -120^\circ & 1\angle 120^\circ \end{bmatrix} * \begin{bmatrix} Y_a \\ Y_b \\ Y_c \end{bmatrix}$$

$$Y_{b1} = 1\angle -120^\circ * Y_{a1}$$
$$Y_{c1} = 1\angle 120^\circ * Y_{a1}$$
$$Y_{b2} = 1\angle -120^\circ * Y_{a2}$$
$$Y_{c2} = 1\angle 120^\circ * Y_{a2}$$

where: Y_a is the phase a voltage or current vector at a specific frequency

Y_b is the phase b voltage or current vector at a specific frequency

Y_c is the phase c voltage or current vector at a specific frequency

Y_{a1} is the positive sequence component of Y_a

Y_{b1} is the positive sequence component of Y_b

Y_{c1} is the positive sequence component of Y_c

Y_{a2} is the negative sequence component of Y_a

Y_{b2} is the negative sequence component of Y_b

Y_{c2} is the negative sequence component of Y_c

Once the sequence harmonic components present in the voltages and currents are known, an impedance profile of the AC network impedance is easily calculated. For each sequence harmonic component, the corresponding impedance can be obtained by taking the ratio of the sequence voltage over the sequence current at that harmonic.

AC network impedance identification can be achieved by continuously sampling the voltage and current and doing FFT analysis while harmonics are being generated on the operating AC system. To realize continuous FFT analysis, the input signals are first passed through anti-aliasing filters to eliminate the higher frequency components in the signals. At each sampling instant the input signals are then decomposed into their frequency components based on sampled data collected during the previous NT seconds (the fundamental period of the input signals). A benefit of this identification technique is the immediacy of results. An AC network impedance profile is generated at each sampling instant. One disadvantage of continuous FFT analysis is loss of continuity of information. At each sampling instant sampled data collected before the previous NT seconds is discarded and a new set of sampled data is used to decompose the input signal into its frequency components. Another disadvantage of this identification technique is the use of a low sampling rate. The sampling rate is set at twice the highest frequency component in the filtered input signal, in accordance with Shannon's sampling theorem [11]. Software models of FFT analysis procedures often use this low sampling rate, as these models were developed for use in protection relay algorithms. When used in protection studies, this sampling rate enables fast extraction of reasonably accurate information [15]. FFT analysis could have been completed using a higher sampling rate. However, the computations involved in FFT analysis increase substantially as the number of samples increase. This can be seen be examining the FFT computational process.

Looking at the decomposition-in-time, radix-2 FFT, the number of complex multiplications required is given by [11]:

$$\frac{N}{2}(\log_2 N)$$

where: N is the number of sampling instances per fundamental period of the input signal

The chosen sampling rate ensures all FFT computations are completed during the time between samples.

A second approach to AC network impedance identification involves sampling the voltage and current over a NT second band of time that occurs while harmonics are being generated on the operating AC system. DFT analysis can then be used to decompose the voltage and current into their frequency components. A disadvantage of this identification technique is the delay in obtaining an impedance profile. After the input signals are sampled and the data is stored, a finite amount of time is required to process the data using DFT analysis. However, an advantage of this technique is the use of an extremely high sampling rate.

Chapter 3: Calculating the Impedance Profile of an AC Network at a HVDC Link

As discussed in Chapter 2, there are various approaches to AC network impedance identification at a HVDC link and there are a variety of ways in which the impedance profile can be calculated from measured system data. The specific approaches researched for this thesis are now discussed and the theory behind impedance profiling via firing angle modulation is presented.

3.1 Approach Taken to Impedance Identification

The research completed for this thesis focuses on the feasibility of measuring the AC network impedance at the HVDC inverter via modulation of the HVDC inverter firing angle signal. A major advantage of this method is that the AC network impedance measurement can be carried out while the impedance is connected to the operating power system. The modulation signal is added to the firing angle control signal while the power system is in operation. The technique that is developed here could be tested and implemented on an actual power system, without disconnecting the AC network impedance. This testing and implementation is left for future study work.

3.1.1 *Software Models of Power Systems and HVDC Controls*

The Power System Computer Aided Design/Electromagnetic Transients Direct Current (PSCAD/EMTDC) computer software program was used to conduct the research for this thesis. Two PSCAD/EMTDC power systems models were used to investigate impedance identification. First, a simplified model of a HVDC link was created. This model includes a detailed model of the HVDC inverter with the rectifier modeled as a DC voltage source. The HVDC controls are not modeled – instead a constant firing angle control signal is assumed. Figure 1 shows a schematic of the simplified HVDC link model.

Figure 1: Schematic of the Simplified HVDC Link Model

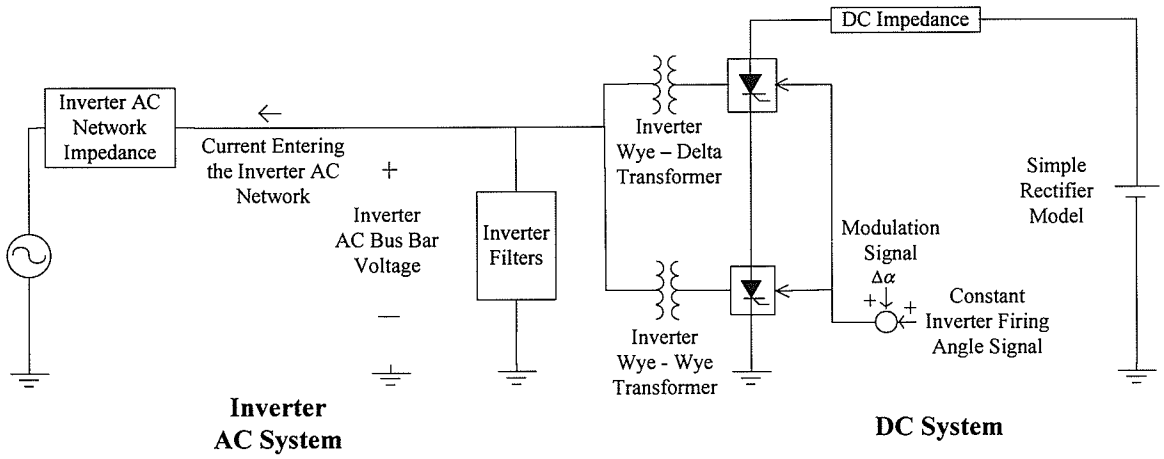

The next HVDC link model to be used was a benchmark model proposed by International Council on Large Electric Systems (CIGRE) [12]. CIGRE has established this benchmark model for HVDC studies. The model manifests many of the operating concerns of typical HVDC systems worldwide and includes a detailed model of the

HVDC rectifier, the HVDC inverter and the HVDC control system. A schematic of the CIGRE benchmark model is shown in Figure 2.

Figure 2: Schematic of the CIGRE HVDC Link Benchmark Model

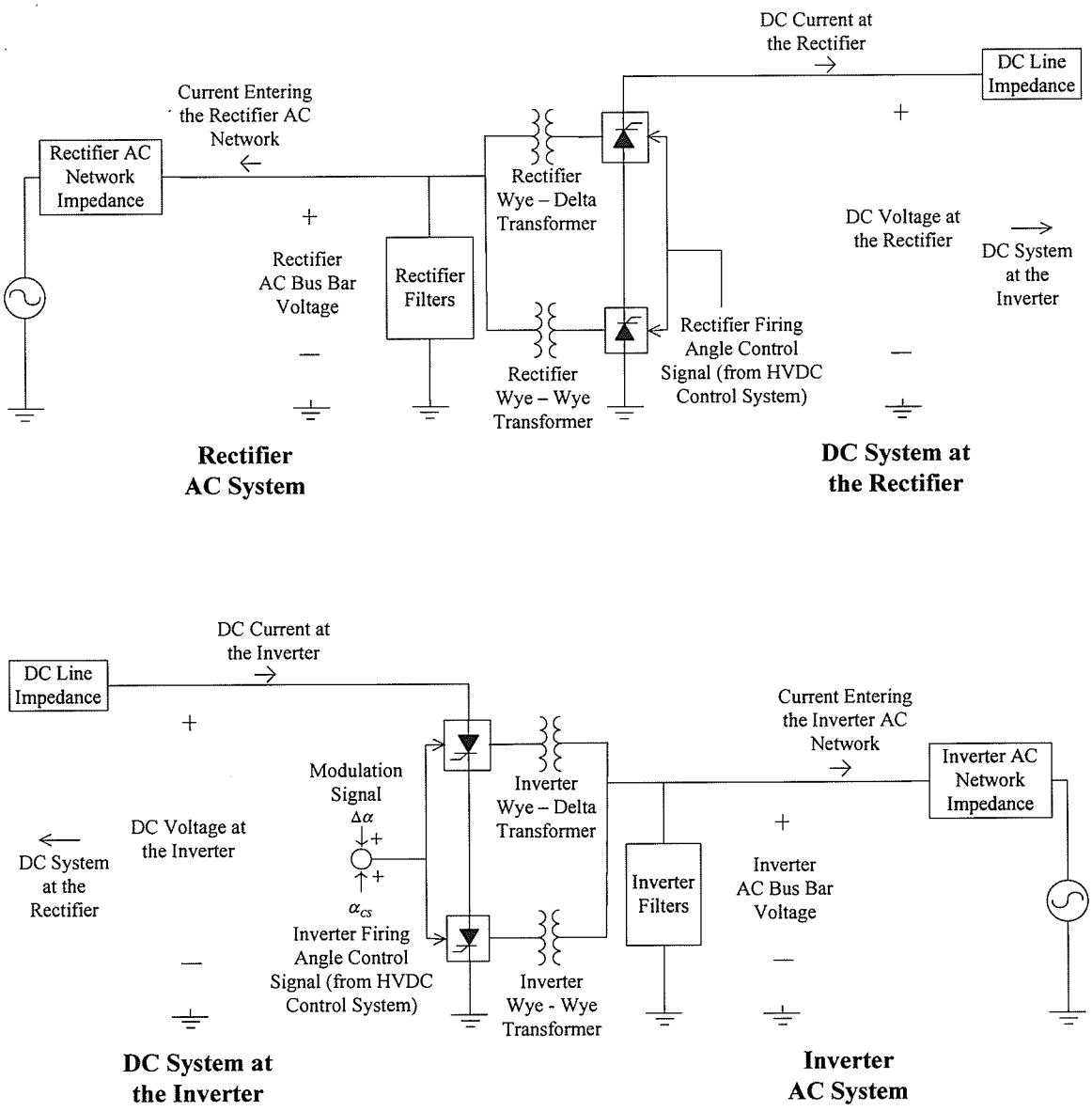

Figure 3 shows a block diagram of the HVDC control system.

Figure 3: Block Diagram of the CIGRE HVDC Link Benchmark Model Control System

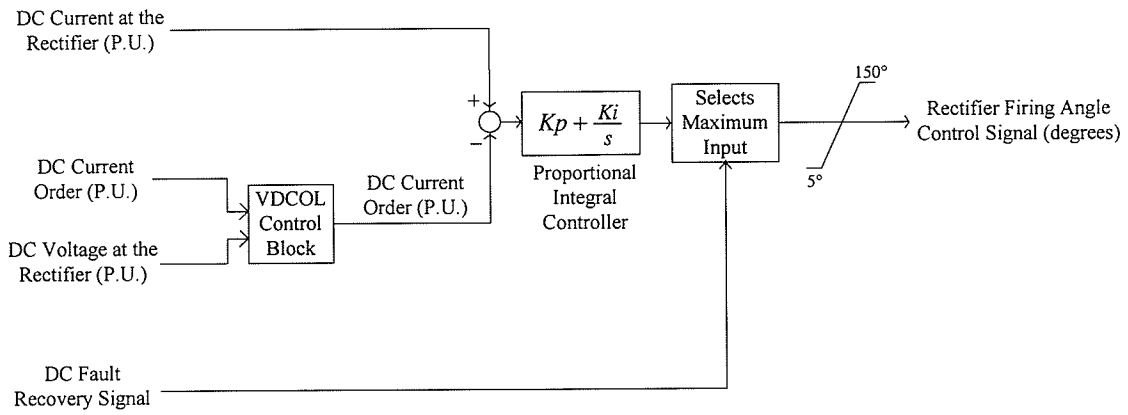

Rectifier Firing Angle Control System

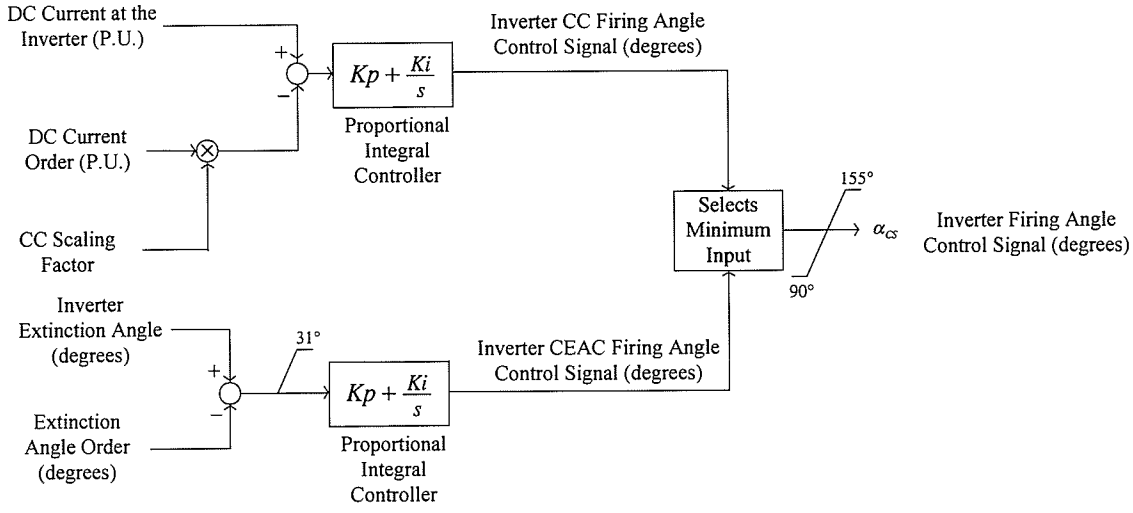

Inverter Firing Angle Control System

The rectifier control system controls the DC current magnitude during normal system operation. This control mode, known as current control (CC), is implemented with a proportional integral controller which attempts to change the rectifier firing angle to maintain a zero error between the DC current at the rectifier and DC current order.

The DC current order input to the rectifier control system is sometimes overridden via the voltage dependent current order limit (VDCOL) control block when the DC voltage at the rectifier drops. The VDCOL control block reduces the chance of thyristor valve damage during a commutation failure. In an attempt to prevent valve overheating during a commutation failure, the VDCOL block outputs a 0.33 P.U. DC current order when the DC voltage at the rectifier is 0.4 P.U. or lower. When the DC voltage at the rectifier is greater than 0.4 P.U., the VDCOL block does not alter the DC current order input.

Unlike AC line faults, DC line faults cannot be cleared by breaker operation because there is no natural zero crossing of DC current that would enable a breaker to open. When a DC line fault occurs, the rectifier firing angle control system facilitates fault clearing by transiently ramping the rectifier firing angle into the inverter firing angle range ($90° - 180°$). This rapidly removes energy from the fault and forces it out to the AC systems at the rectifier and inverter. The DC fault recovery signal is set to a high positive value when a DC line fault occurs and remains at this value for 0.15 seconds. At all other times this signal is set to a negative value.

During normal system operation, the inverter control system controls the inverter extinction angle γ. This γ is the extinction angle of the inverter thyristor valves. The extinction angle specifies the duration of time from the extinguishing of current flow through the thyristor valves to the subjection of the thyristor valves to a forward biasing voltage [7, 8]. It is critically important to ensure the inverter extinction angle does not fall below the inverter minimum extinction angle γ_{min} [7, 8]. The turn-off time of a thyristor valve is the time required for the valve to reestablish its current blocking ability after the current through the valve is extinguished [7]. The inverter minimum extinction angle is defined as:

$$\gamma_{min} = f_o * t_{off}$$

where: t_{off} is the turn-off time of the inverter thyristor valves [8]

At the same time, it is important to ensure the smallest possible inverter extinction angle so that the reactive power consumed by the HVDC inverter is minimized [8]. Hence, during normal operation the inverter control system attempts to keep the inverter extinction angle constant at a fixed value known as the extinction angle order. The extinction angle order is typically set at 15° - 20° [7]. This control mode is called constant extinction angle control (CEAC) and is implemented with a proportional integral controller which attempts to change the inverter firing angle to maintain a zero error between the inverter extinction angle and the extinction angle order.

When a system transient or disturbance occurs, the rectifier AC voltage magnitude may drop and the rectifier control system may be unable to effectively control the DC current magnitude [8]. When the rectifier cannot push sufficient current through the DC line, the inverter control system enters a backup constant current (CC) control mode to prevent DC system collapse and allow for a degraded mode of DC system operation [8]. The backup CC control is implemented with a proportional integral controller which attempts to change the inverter firing angle to maintain a zero error between the DC current at the inverter and a set fraction of the DC current order. This set fraction, the CC scaling factor, is typically set to 0.9 [8].

3.1.2 Modulation of the HVDC Inverter Firing Angle Signal

The research completed for this thesis investigates the feasibility of measuring the AC network impedance at the HVDC inverter via modulation of the HVDC inverter firing angle signal. Both single frequency and multiple frequency sinusoidal modulation signals were considered. These two types of modulation signals were introduced and described in section 2.2.

3.1.2.1 Single Frequency Sinusoidal Modulation of the Firing Angle Signal

The first attempt to measure the AC network impedance involved adding a single frequency sinusoidal modulation signal to the firing angle control signal in the simplified HVDC link model. The modulation magnitude was easily chosen to produce detectable and measurable AC harmonics without disturbing system operation. The modulation frequency was varied over a wide frequency range to determine various AC network impedance profiles. This involved separately injecting a large number of firing angle modulation signals. Many computer simulations were necessary, requiring a large amount of time and effort.

3.1.2.1 Multiple Frequency Sinusoidal Modulation of the Firing Angle Signal

The bulk of the thesis research work involved the use of multiple frequency sinusoidal modulation signals with both the simplified and the CIGRE benchmark model of a HVDC link. The modulation signals were carefully chosen so as not to significantly affect system operation while modulation took place. This involved limiting the magnitude of each sinusoidal component and phase staggering each sinusoidal component by a chosen amount [1] in the modulation signals.

Consider the firing angle modulation signal given below:

$$\Delta\alpha = \sum_{b=1}^{bm} A * \sin(2\pi bt)$$

where: t is the time

With A = 0.1° and bm = 350, this signal has a fundamental frequency of 1 Hz and contains frequency components at 1, 2, 3,..., 350 Hz. It has bunches of spikes in magnitude that occur every second, as shown in Figure 4. Similar to an impulse signal, this modulation signal would be very disruptive to the control and operation of a HVDC link.

Figure 4: Firing Angle Modulation Signal Without Phase Staggered Frequency Components

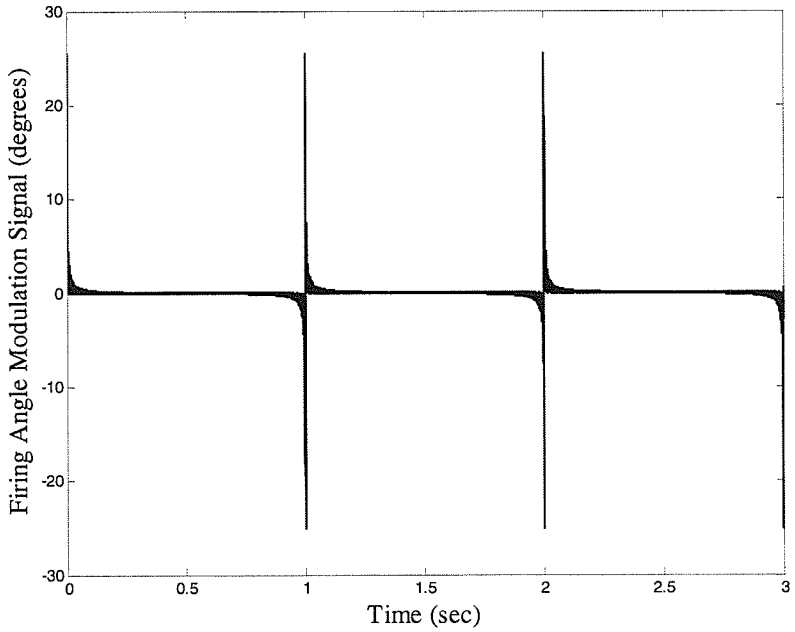

In an attempt to improve the previous firing angle modulation signal so that the bunching effect is minimized, the following signal [1] was considered.

$$\Delta\alpha = \sum_{b=1}^{bm} A * \sin(2\pi bt + \frac{\pi}{180}(b-1)^m)$$

where: m is the phase staggering exponent

With A = 0.1°, bm = 350 and m = 2, this signal also has a fundamental frequency of 1 Hz and contains frequency components at 1, 2, 3,..., 350 Hz. However, the phase of each frequency component in the signal has been staggered. As shown in Figure 5, this signal does not contain large spikes and could be used as a firing angle modulation signal without disrupting the control and operation of a HVDC link. Such a suitable modulation signal can be obtained with m = 2, 3, 4,....

Figure 5: Firing Angle Modulation Signal With Phase Staggered Frequency Components

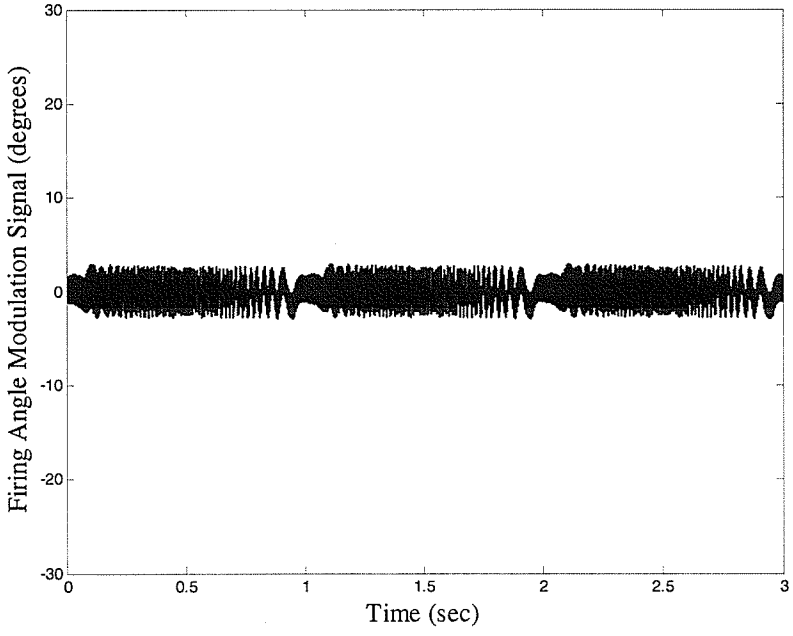

In addition to limiting the magnitude of each sinusoidal component and phase staggering each sinusoidal component in the modulation signals, when using the CIGRE benchmark model with the HVDC control system in operation, the numbers of frequencies in the multiple frequency modulation signals were limited to ensure the modulation did not significantly affect system operation.

Using multiple frequency sinusoidal modulation signals, various AC network impedance profiles were calculated at many system operating points. The profiles were determined over a specific frequency range. When using the CIGRE benchmark model with the HVDC control system in operation, this involved injecting more than one multiple frequency sinusoidal modulation signal. In all cases impedance profiling was completed quite quickly.

3.1.3 FFT and DFT Network Impedance Identification Techniques

The Fast Fourier Transform (FFT) and Discrete Fourier Transform (DFT) impedance identification techniques were introduced and described in section 2.3. When single frequency sinusoidal modulation signals were injected, impedance profiles were obtained using a FFT technique with low sampling frequency. When multiple frequency sinusoidal modulation signals were injected, impedance profiles were obtained using both FFT (low sampling frequency) and DFT (high sampling frequency) impedance identification techniques. This allowed for direct comparison of the two methods to determine the optimal identification technique.

Using the FFT technique, AC network impedance identification was achieved by first removing the fundamental frequency components from the AC bus bar voltage and current entering the AC network. During single frequency modulation, the resulting voltages and currents were then filtered to keep the most significant harmonics produced by the modulation. During multiple frequency modulation, the resulting voltages and currents were filtered to remove all frequency components outside the frequency range of interest. The filtered voltages and currents were passed through anti-aliasing filters and were then constantly sampled. FFT analysis was used to decompose the filtered voltage and current into their frequency components. This FFT analysis, as well as sequence component extraction, was conducted continuously while harmonics were being generated on the operating AC system. An impedance profile was immediately calculated.

Using the DFT technique, AC network impedance identification was achieved using a program written in Matlab computer software. The AC bus bar voltage and current entering the AC network were monitored while harmonics were generated on the AC system. The voltage and current data were then input to the Matlab DFT program. This program performs DFT analysis to decompose the voltage and current into their frequency components. It then breaks down each frequency component into its sequence components to calculate an impedance profile.

3.2 Theory of Impedance Profiling via Firing Angle Modulation

As previously mentioned, this thesis investigates the feasibility of measuring the AC network impedance at the HVDC inverter via modulation of the HVDC inverter firing angle signal. The modulation signal is added to the firing angle control signal while the power system is in operation.

Consider the following single frequency sinusoidal modulation signal:

$$\Delta\alpha = k_\upsilon * \sin(\upsilon t + \phi_\upsilon)$$

where: k_υ is the magnitude of the modulation signal

υ is the frequency of the modulation signal

ϕ_υ is the phase of the modulation signal

Then

$$\alpha = \alpha_{cs} + \Delta\alpha = \alpha_{cs} + k_\upsilon * \sin(\upsilon t + \phi_\upsilon)$$

where α_{cs} is the firing angle control signal prior to the addition of the modulation signal

At the 12-pulse HVDC inverter

$$V_{dc} = \frac{6\sqrt{2}}{\pi} * V_l * \cos\gamma - \frac{3}{\pi} * X_c * I_{dc}$$

and

$$\alpha + \mu + \gamma = 180°$$

where: V_{dc} is the DC voltage

V_l is the fundamental inverter AC bus bar voltage referred to the secondary side of the inverter transformers (RMS, line-line quantity)

γ is the extinction angle

X_c is the commutating reactance of the inverter transformers

I_{dc} is the DC current

μ is the overlap angle [8]

For a small commutating reactance $X_c \approx 0$, $\mu \approx 0$ and the subsequent simplified equations apply:

$$\alpha + \gamma = 180°$$

and

$$V_{dc} = \frac{6\sqrt{2}}{\pi} * V_l * \cos\gamma = -\frac{6\sqrt{2}}{\pi} * V_l * \cos\alpha$$

With single frequency sinusoidal modulation

$$V_{dc} = -\frac{6\sqrt{2}}{\pi} * V_l * \cos(\alpha_{cs} + k_\upsilon * \sin(\upsilon t + \phi_\upsilon))$$

Now, consider the $\cos(\alpha_{cs} + k_v * \sin(\upsilon t + \phi_v))$ portion of V_{dc}. Using a trigonometric identity [16]:

$$\cos(\alpha_{cs} + k_v * \sin(\upsilon t + \phi_v)) = \cos(\alpha_{cs}) * \cos(k_v * \sin(\upsilon t + \phi_v)) - \sin(\alpha_{cs}) * \sin(k_v * \sin(\upsilon t + \phi_v))$$

The Maclaurin series expansion of a function g(x) is [16]:

$$g(x) = g(0) + g'(0) + \frac{g''(0) * x^2}{2!} + \frac{g'''(0) * x^3}{3!} + \ldots$$

Therefore

$$\cos(x) = 1 - \frac{x^2}{2!} + \frac{x^4}{4!} - + \ldots \text{ and } \sin(x) = x - \frac{x^3}{3!} + \frac{x^5}{5!} - + \ldots$$

which gives

$$\cos(k_v * \sin(\upsilon t + \phi_v)) = 1 - \frac{{k_v}^2 * \sin^2(\upsilon t + \phi_v)}{2} + \frac{{k_v}^4 * \sin^4(\upsilon t + \phi_v)}{24} - + \ldots$$

and

$$\sin(k_v * \sin(\upsilon t + \phi_v)) = k_v * \sin(\upsilon t + \phi_v) - \frac{{k_v}^3 * \sin^3(\upsilon t + \phi_v)}{6} + \frac{{k_v}^5 * \sin^5(\upsilon t + \phi_v)}{120} - + \ldots$$

To ensure system operation is not disturbed, the modulation magnitude, k_v, will be small. For small k_v, it can be assumed that:

$$\cos(k_v * \sin(\upsilon t + \phi_v)) = 1 - \frac{{k_v}^2 * \sin^2(\upsilon t + \phi_v)}{2}$$

and

$$\sin(k_v * \sin(\upsilon t + \phi_v)) = k_v * \sin(\upsilon t + \phi_v)$$

Using a trigonometric identity [16]

$$\cos(k_\upsilon * \sin(\upsilon t + \phi_\upsilon)) = 1 - \frac{{k_\upsilon}^2 * \sin^2(\upsilon t + \phi_\upsilon)}{2} = 1 - \frac{{k_\upsilon}^2}{2} * \left(\frac{1 - \cos(2\upsilon t + 2\phi_\upsilon)}{2} \right)$$

Consequently

$$\cos(k_\upsilon * \sin(\upsilon t + \phi_\upsilon)) = 1 - \frac{{k_\upsilon}^2}{2} * \left(\frac{1 - \cos(2\upsilon t + 2\phi_\upsilon)}{2} \right) = 1 - \frac{{k_\upsilon}^2}{4} + \frac{{k_\upsilon}^2}{4} * \cos(2\upsilon t + 2\phi_\upsilon))$$

and

$$\cos(\alpha_{cs} + k_\upsilon * \sin(\upsilon t + \phi_\upsilon)) = \cos(\alpha_{cs}) * \cos(k_\upsilon * \sin(\upsilon t + \phi_\upsilon)) - \sin(\alpha_{cs}) * \sin(k_\upsilon * \sin(\upsilon t + \phi_\upsilon))$$

$$= \cos(\alpha_{cs}) * \left(1 - \frac{{k_\upsilon}^2}{4} + \frac{{k_\upsilon}^2}{4} * \cos(2\upsilon t + 2\phi_\upsilon) \right) - \sin(\alpha_{cs}) * k_\upsilon * \sin(\upsilon t + \phi_\upsilon)$$

Since

$$V_{dc} = -\frac{6\sqrt{2}}{\pi} * V_l * \cos(\alpha_{cs} + k_\upsilon * \sin(\upsilon t + \phi_\upsilon)),$$

the DC voltage can be expressed as follows:

$$V_{dc} = -\frac{6\sqrt{2}}{\pi} * V_l * \cos(\alpha_{cs}) * \left(1 - \frac{{k_\upsilon}^2}{4} + \frac{{k_\upsilon}^2}{4} * \cos(2\upsilon t + 2\phi_\upsilon) \right) + \frac{6\sqrt{2}}{\pi} * V_l * k_\upsilon * \sin(\alpha_{cs}) * \sin(\upsilon t + \phi_\upsilon)$$

$$= -\frac{6\sqrt{2}}{\pi} * V_l * \left(\left(1 - \frac{{k_\upsilon}^2}{4} \right) * \cos(\alpha_{cs}) + \frac{{k_\upsilon}^2}{4} * \cos(\alpha_{cs}) * \cos(2\upsilon t + 2\phi_\upsilon) - k_\upsilon * \sin(\alpha_{cs}) * \sin(\upsilon t + \phi_\upsilon) \right)$$

$$= -\frac{6\sqrt{2}}{\pi} * V_l * \left(\left(1 - \frac{{k_\upsilon}^2}{4} \right) * \cos(\alpha_{cs}) - k_\upsilon * \sin(\alpha_{cs}) * \sin(\upsilon t + \phi_\upsilon) + \frac{{k_\upsilon}^2}{4} * \cos(\alpha_{cs}) * \cos(2\upsilon t + 2\phi_\upsilon) \right)$$

Therefore, modulating the firing angle signal with a small sinusoidal signal of frequency υ will produce harmonics on the DC system at frequency υ and at frequency 2υ.

Furthermore, these DC system harmonics will produce harmonics on the inverter AC system, modulating the amplitudes of the fundamental voltages and currents [7, 6]. A DC harmonic at frequency υ results in a positive sequence AC harmonic at frequency ($\upsilon + f_o$) and a negative sequence AC harmonic at frequency ($\upsilon - f_o$). Similarly, a DC harmonic at frequency 2υ results in a positive sequence AC harmonic at frequency ($2\upsilon + f_o$) and a negative sequence AC harmonic at frequency ($2\upsilon - f_o$). Consequently, the resulting frequency spectrums of AC system voltages and currents will contain double side-band components at ($\upsilon \pm f_o$) and at ($\upsilon \pm 2 f_o$) as well as fundamental frequency components.

For small k_υ, the DC harmonic at frequency 2υ is much smaller than the DC harmonic at frequency υ and hence can be neglected. Therefore, the most significant harmonic voltages and currents produced on the AC system are a positive sequence harmonic at frequency ($\upsilon + f_o$) and a negative sequence harmonic at frequency ($\upsilon - f_o$).

The previous analysis, which assumed a small single frequency modulation signal, is valuable even when the modulation signal is a small multiple frequency sinusoidal signal. Superposition is valid when the multiple frequency modulation signal does not cause a significant system disturbance. It follows that the harmonic voltages and currents produced on the AC system by the multiple frequency modulation signal will be the sum of the harmonic voltages and currents produced from each of the sinusoidal frequency components in the modulation signal.

Chapter 4: Calculation of an Impedance Profile – Simulation Results

This thesis investigates the feasibility of AC network impedance measurement via single and multiple frequency sinusoidal modulation of the HVDC inverter firing angle signal. Using single frequency sinusoidal modulation, the modulation magnitude can be easily chosen to produce detectable and measurable AC harmonics without disturbing system operation. However, the modulation frequency must be varied over a wide frequency range to determine an AC network impedance profile. This involves separately injecting a large number of firing angle modulation signals, which requires a large amount of time and effort. When using multiple frequency sinusoidal modulation the modulation signal must be carefully chosen so as not to disturb system operation. Using this type of modulation signal, it is possible to generate an accurate impedance profile over a specific frequency band and this accurate impedance profile can be generated many times faster than could be accomplished using single frequency modulation.

Two methods are used in calculating the impedance profiles – a Fast Fourier Transform (FFT) method and a Discrete Fourier Transform (DFT) method. With the FFT method, immediate impedance identification is achieved by constantly sampling the filtered AC bus bar voltage and current entering the AC network. The filtered voltage and current signals are sampled at twice the highest frequency component in the signals, in accordance with Shannon's sampling theorem. FFT analysis is conducted continuously while harmonics are being generated on the operating AC system. With continuous FFT analysis, there is loss of continuity of information. At each sampling instant a new set of sampled data is used and the previous set of data is discarded. With the DFT method, impedance identification is achieved by sampling the AC bus bar voltage and current entering the AC network for a period of time while harmonics are being generated on the operating AC system. DFT analysis is used to decompose the voltage and current into their frequency components. This decomposition requires a finite amount of time. When doing DFT analysis, the voltage and current can be sampled at an extremely high rate.

Simulation and test results are presented in this chapter. As mentioned in section 1.2, the accuracy of the chosen impedance profiling methods was tested for various network impedances and DC current orders. Using a simplified model of a HVDC link,

impedance profiles were generated for resistive-inductive (RL), RRL, RLL and resistive-resistive-inductive-inductive-capacitive (RRLLC) type impedances. In addition, impedance profiles were generated for weak and strong inverter AC networks using an International Council on Large Electric Systems (CIGRE) benchmark model of a HVDC link [12]. Using the CIGRE model, impedance profiles were taken at various DC current orders to test the profiling methods under different DC line loading conditions. The impact of a HVDC control system on impedance profiling was also investigated using the CIGRE benchmark model.

4.1 Software Models of AC Network Impedances

An actual power system could have an arbitrary AC network impedance. As mentioned in section 1.1, this impedance affects the commutating voltage of the HVDC link, which in turn affects the performance of the link and the overall behavior of the system. The strength of the AC system is quantified by the Short Circuit Ratio (SCR) and the Effective Short Circuit Ratio (ESCR). However, the SCR and ESCR are calculated only at the fundamental frequency of the AC system. Consequently, these ratios do not accurately reflect the transient behavior of the AC network impedance. In HVDC studies, the network impedance is modeled to capture the desired higher frequency behavior of the network as well as the desired strength of the system. The network impedance is typically modeled as a simple RL, RRL, RLL or RRLLC type impedance. Accordingly, in completing the research work for this thesis, impedance profiling methods were tested using RL, RRL, RLL and RRLLC type impedances as well as weak

and strong AC systems. Figure 6 shows schematic diagrams of the various AC network impedance models used to test the chosen impedance profiling methods.

Figure 6: Schematic Diagrams of the AC Network Impedance Models

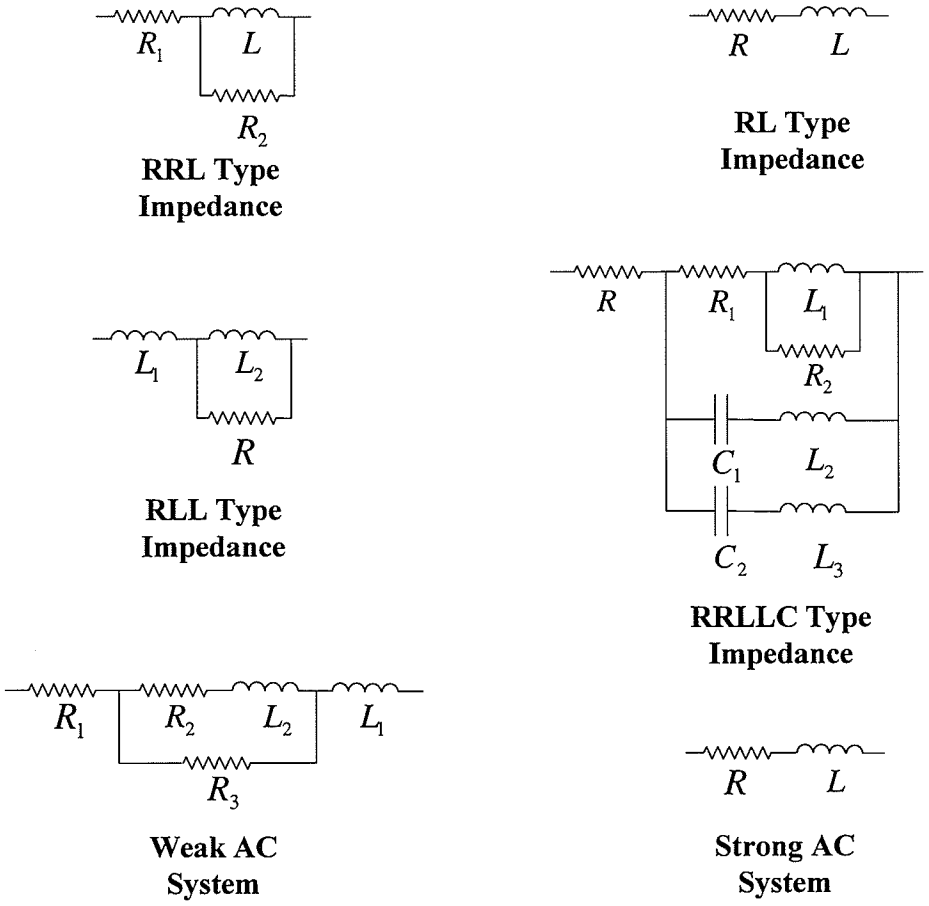

4.2 Applying the Impedance Profiling Methods to a Simplified Model of a HVDC Link

The simplified HVDC link model includes a detailed model of the HVDC inverter with the rectifier modeled as a DC voltage source. The HVDC controls are not modeled – instead a constant firing angle control signal is assumed. Figure 1 shows a schematic of the simplified HVDC link model.

To begin, a single frequency sinusoidal modulation signal was added to the firing angle control signal in the simplified HVDC link model. A modulation magnitude of 0.2° was chosen as this magnitude produced detectable and measurable AC harmonics without causing noticeable disturbance on the AC system. With the fundamental frequency of the AC system set at 60 Hz, positive sequence impedance profiles were calculated over the 10-400 Hz frequency band by injecting a number of separate firing angle modulation signals with the following frequencies: 10, 20, 30,..., 340 Hz. In each case, a 50 μ s time step was used and firing angle modulation was conducted for 2 seconds. For each modulation signal, AC network impedance identification was achieved using the FFT technique. First, the fundamental frequency components from the AC bus bar voltage and current entering the AC network were removed. The resulting voltages and currents were then filtered to keep the most significant harmonics produced by the modulation. The filtered voltages and currents were passed through anti-aliasing filters and were continuously sampled. FFT analysis and positive sequence component extraction was carried out continuously over the 2 second modulation period. The results given in

section 4.2.1 for single frequency sinusoidal modulation are based on impedance profiles obtained near the end of the 2 second modulation period.

Next, a multiple frequency sinusoidal modulation signal was added to the firing angle control signal in the simplified HVDC link model. With the fundamental frequency of the AC system set at 60 Hz, positive sequence impedance profiles were calculated over the 10-400 Hz frequency band by injecting multiple frequency modulation signals with the following frequencies: 10, 20, 30,..., 340 Hz. In each case, firing angle modulation was conducted for 3 seconds. The multiple frequency sinusoidal modulation signals were carefully chosen to produce detectable and measurable AC harmonics without causing noticeable disturbance on the AC system. The magnitude of each sinusoidal component in the modulation signals varies between $0.02°$ and $0.14°$. Each sinusoidal component was phase staggered – a phase staggering exponent of 5 or 8 was used. This ensures no multiple frequency modulation signal has a magnitude exceeding $1.31°$. With the time step set to 50 μ s, AC network impedance identification was achieved using the FFT technique. First, the AC bus bar voltage and current entering the AC network were filtered. The fundamental frequency components and all frequency components outside the 5-405 Hz frequency range were removed. The filtered voltage and current were passed through anti-aliasing filters and were continuously sampled. FFT analysis was carried out continuously over the 3 second modulation period. Also, the positive sequence component was extracted from each frequency component throughout the modulation period. The results given in section 4.2.1 for impedance identification using

the FFT technique and multiple frequency sinusoidal modulation are based on impedance profiles obtained near the end of the 3 second modulation period. With the time step set to 10 μ s, AC network impedance identification using the DFT technique was achieved through use of the Matlab DFT program. The AC bus bar voltage and current entering the AC network were monitored throughout the 3 second modulation period. A 0.1 second portion of this voltage and current data (obtained near the end of the 3 second modulation period) was then input to the Matlab DFT program. This program performed DFT analysis on the voltage and current and then extracted the positive sequence component from each frequency component to calculate a positive sequence impedance profile of the AC network.

All impedance profiles displayed in section 4.2.1 are positive sequence impedance profiles. Also, the calculated impedance profile is always shown as a dotted line and the actual impedance profile is always shown as a solid line.

4.2.1 Testing the Impedance Profiling Methods using Various Network Impedances

In HVDC system studies, the AC network impedance is typically modeled as a RL, RRL, RLL or RRLLC type impedance. The high frequency behaviors of these impedance types characterize high frequency behaviors commonly seen in actual power systems. Using the simplified model of a HVDC link, the impedance profiling methods were tested for RL, RRL, RLL and RRLLC type impedances, as shown in Figure 6. For each impedance type, the addition of a single frequency sinusoidal modulation signal to the inverter firing angle control signal produced negligible disturbance on the AC system. In addition, multiple frequency sinusoidal modulation of the firing angle control signal did not ever significantly disturb the AC system.

4.2.1.1 AC Network Impedance: RL

The first AC network impedance type to be profiled was a RL type impedance as shown in Figure 6. The RL impedance model has a 1.71 Ω resistive component and a 0.026 H inductive component.

The impedance profile obtained by completing AC network impedance identification using the FFT technique and single frequency sinusoidal modulation is shown in Figure 7 and Figure 8. The calculated impedance profile is very accurate over the 10-400 Hz frequency range.

When the multiple frequency sinusoidal modulation signal was added to the firing angle control signal, the amplitude of the fundamental AC bus bar voltage was modulated by 1.1 kV (0.6% of the fundamental amplitude) and the amplitude of the fundamental current entering the AC network was modulated by 0.05 kA (2.3% of the fundamental amplitude).

The impedance profile obtained by completing AC network impedance identification using the FFT technique and multiple frequency sinusoidal modulation is shown in Figure 9 and Figure 10. There are some inaccuracies in the calculated impedance profile at 10 Hz and 40 Hz and around the 90 Hz, 150 Hz, 200 Hz and 350 Hz frequencies.

Figure 11 and Figure 12 show the impedance profile obtained by completing AC network impedance identification using the DFT technique and multiple frequency sinusoidal modulation. The calculated impedance profile is very accurate over the 10-400 Hz frequency range.

Figure 7: RL Impedance Magnitude Profile - Single Frequency Sinusoidal Modulation using the FFT Technique

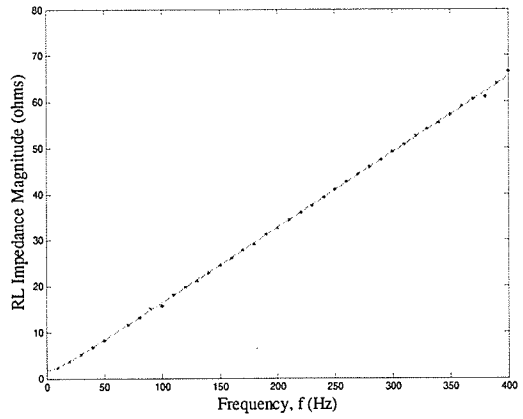

Figure 8: RL Impedance Phase Profile - Single Frequency Sinusoidal Modulation using the FFT Technique

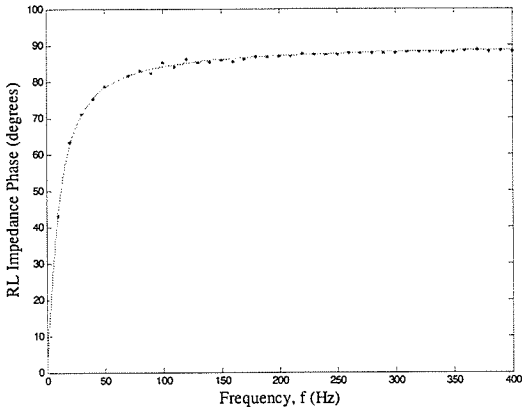

Figure 9: RL Impedance Magnitude Profile - Multiple Frequency Sinusoidal Modulation using the FFT Technique

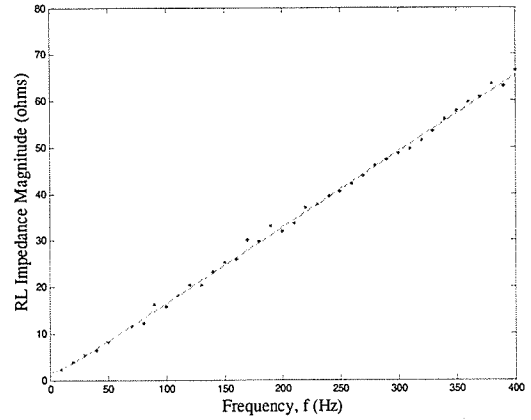

Figure 10: RL Impedance Phase Profile - Multiple Frequency Sinusoidal Modulation using the FFT Technique

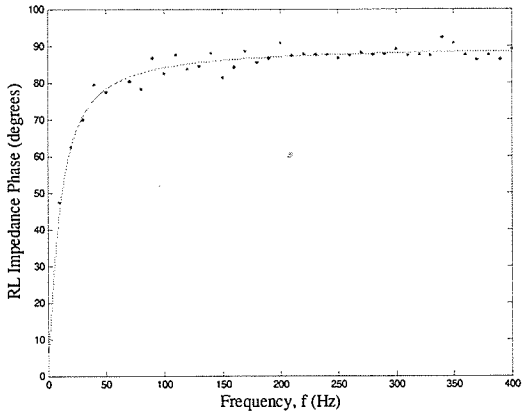

Figure 11: RL Impedance Magnitude Profile - Multiple Frequency Sinusoidal Modulation using the DFT Technique

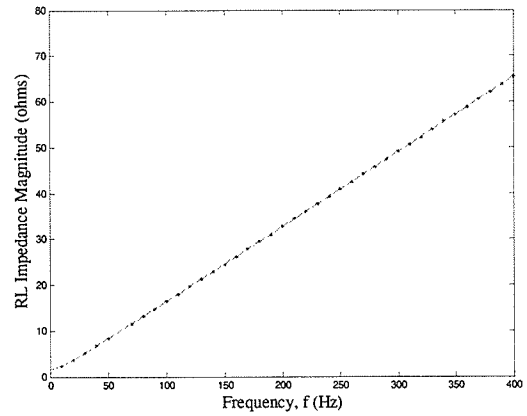

Figure 12: RL Impedance Phase Profile – Multiple Frequency Sinusoidal Modulation using the DFT Technique

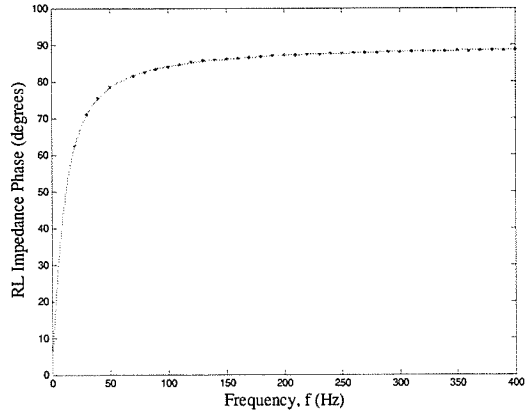

4.2.1.2 AC Network Impedance: RRL

The next AC network impedance type to be profiled was a RRL type impedance as shown in Figure 6. The RRL impedance model has a 0.04 H inductive component. Resistor R_1 has a value of 1.71 Ω and resistor R_2 has a value of 70 Ω.

The impedance profile obtained by completing AC network impedance identification using the FFT technique and single frequency sinusoidal modulation is shown in Figure 13 and Figure 14. The calculated impedance profile is very accurate over the 10-400 Hz frequency range.

When the multiple frequency sinusoidal modulation signal was added to the firing angle control signal, the amplitude of the fundamental AC bus bar voltage was modulated by 0.4 kV (0.2% of the fundamental amplitude) and the amplitude of the fundamental current entering the AC network was modulated by 0.03 kA (1.4% of the fundamental amplitude).

The impedance profile obtained by completing AC network impedance identification using the FFT technique and multiple frequency sinusoidal modulation is shown in Figure 15 and Figure 16. There is some inaccuracy in the calculated impedance phase at 360 Hz and around the 60 Hz frequency.

Figure 17 and Figure 18 show the impedance profile obtained by completing AC network impedance identification using the DFT technique and multiple frequency sinusoidal modulation. The calculated impedance profile is very accurate over the 10-400 Hz frequency range.

Figure 13: RRL Impedance Magnitude Profile - Single Frequency Sinusoidal Modulation using the FFT Technique

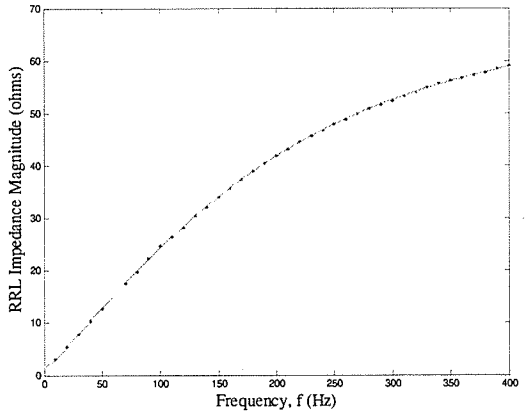

Figure 14: RRL Impedance Phase Profile - Single Frequency Sinusoidal Modulation using the FFT Technique

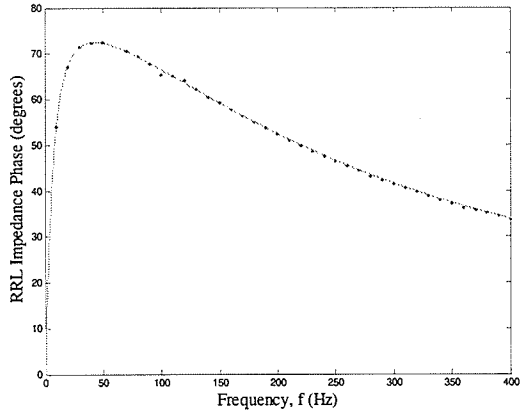

Figure 15: RRL Impedance Magnitude Profile - Multiple Frequency Sinusoidal Modulation using the FFT Technique

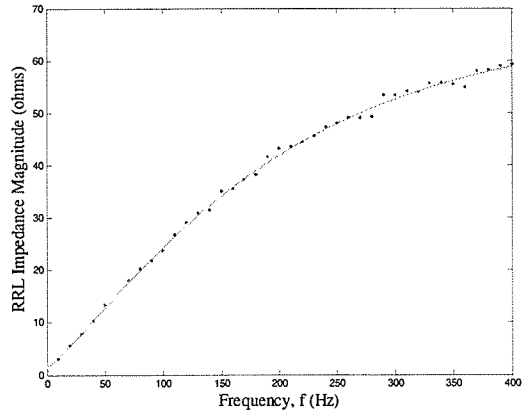

Figure 16: RRL Impedance Phase Profile - Multiple Frequency Sinusoidal Modulation using the FFT Technique

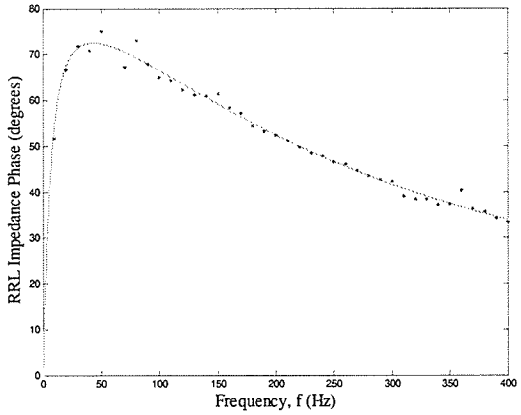

Figure 17: RRL Impedance Magnitude Profile - Multiple Frequency Sinusoidal Modulation using the DFT Technique

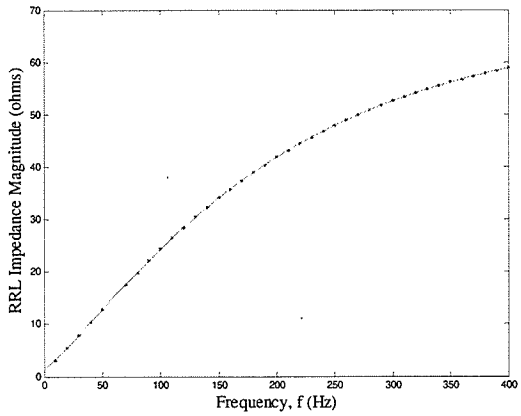

Figure 18: RRL Impedance Phase Profile – Multiple Frequency Sinusoidal Modulation using the DFT Technique

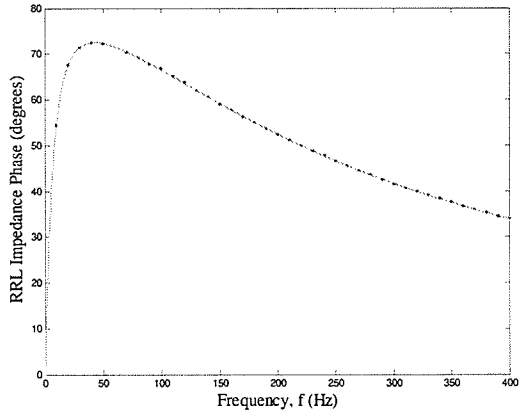

4.2.1.3 AC Network Impedance: RLL

The third AC network impedance type to be profiled was a RLL type impedance as shown in Figure 6. The RLL impedance model has a 0.1 Ω resistive component. Inductor L_1 has a value of 0.035 H and inductor L_2 has a value of 0.01 H.

The impedance profile obtained by completing AC network impedance identification using the FFT technique and single frequency sinusoidal modulation is shown in Figure 19 and Figure 20. Aside from some minor error in the calculated impedance phase at 20 Hz and 90 Hz, the calculated profile is very accurate over the 10-400 Hz frequency range.

When the multiple frequency sinusoidal modulation signal was added to the firing angle control signal, the amplitude of the fundamental AC bus bar voltage was modulated by 1.4 kV (0.8% of the fundamental amplitude) and the amplitude of the fundamental current entering the AC network was modulated by 0.04 kA (2.1% of the fundamental amplitude).

The impedance profile obtained by completing AC network impedance identification using the FFT technique and multiple frequency sinusoidal modulation is shown in Figure 21 and Figure 22. There are some inaccuracies in the calculated impedance profile at 360 Hz and 370 Hz and around the 40 Hz and 80 Hz frequencies.

Figure 23 and Figure 24 show the impedance profile obtained by completing AC network impedance identification using the DFT technique and multiple frequency sinusoidal modulation. Aside from some minor error in the calculated impedance magnitude around the 340 Hz frequency, the calculated profile is very accurate over the 10-400 Hz frequency range.

Figure 19: RLL Impedance Magnitude Profile - Single Frequency Sinusoidal Modulation using the FFT Technique

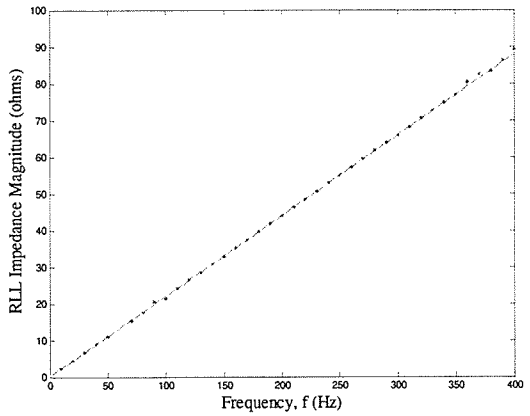

Figure 20: RLL Impedance Phase Profile - Single Frequency Sinusoidal Modulation using the FFT Technique

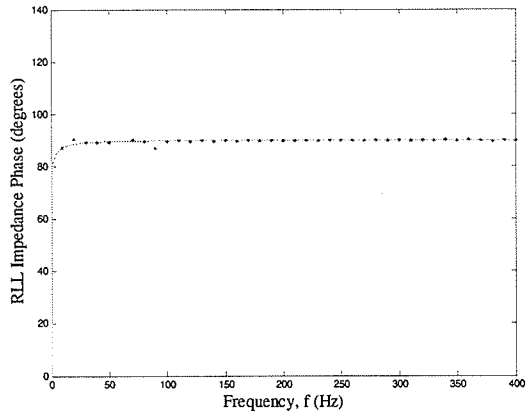

Figure 21: RLL Impedance Magnitude Profile - Multiple Frequency Sinusoidal Modulation using the FFT Technique

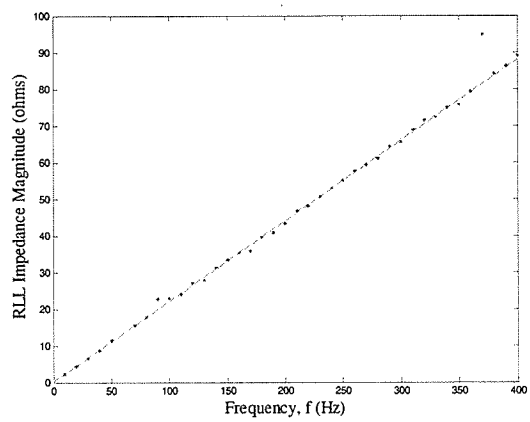

Figure 22: RLL Impedance Phase Profile - Multiple Frequency Sinusoidal Modulation using the FFT Technique

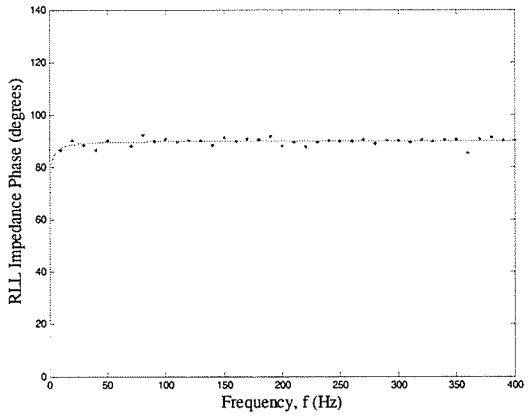

Figure 23: RLL Impedance Magnitude Profile - Multiple Frequency Sinusoidal Modulation using the DFT Technique

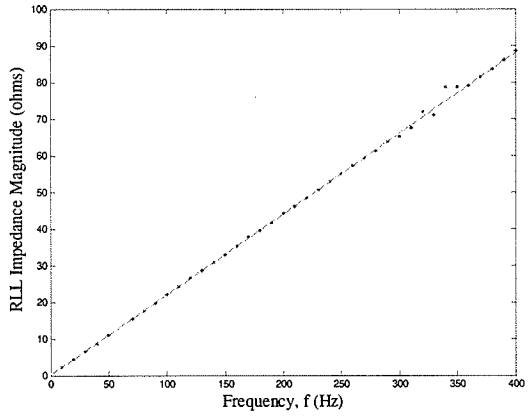

Figure 24: RLL Impedance Phase Profile – Multiple Frequency Sinusoidal Modulation using the DFT Technique

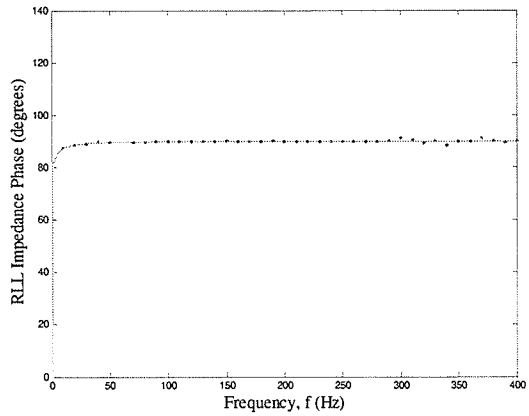

4.2.1.4 AC Network Impedance: RRLLC

The fourth AC network impedance type to be profiled was a RRLLC type impedance as shown in Figure 6. The RRLLC impedance model consists of three parallel branches in series with a 1.71 Ω resistor. Inductors L_1, L_2 and L_3 are set equal to 0.04 H. Capacitor C_1 has a value of 11 μF and C_2 has a value of 3.6 μF. Resistor R_1 has a value of 0.2 Ω and R_2 has a value of 70 Ω. This RRLLC impedance has two resonant frequencies produced by the two series LC branches. Resonant frequencies occur at 240 and 420 Hz.

The impedance profile obtained by completing AC network impedance identification using the FFT technique and single frequency sinusoidal modulation is shown in Figure 25 and Figure 26. Aside from some minor error in the calculated impedance profile around the 360 Hz frequency, the calculated profile is very accurate over the 10-400 Hz frequency range.

When the multiple frequency sinusoidal modulation signal was added to the firing angle control signal, the amplitude of the fundamental AC bus bar voltage was modulated by 0.5 kV (0.3% of the fundamental amplitude) and the amplitude of the fundamental current entering the AC network was modulated by 0.03 kA (1.2% of the fundamental amplitude).

The impedance profile obtained by completing AC network impedance identification using the FFT technique and multiple frequency sinusoidal modulation is shown in Figure 27 and Figure 28. There are some inaccuracies in the calculated impedance profile at 70 Hz, 360 Hz and 400 Hz and around the 210 Hz and 280 Hz frequencies.

Figure 29 and Figure 30 show the impedance profile obtained by completing AC network impedance identification using the DFT technique and multiple frequency sinusoidal modulation. The calculated impedance profile is very accurate over the 10-400 Hz frequency range.

Figure 25: RRLLC Impedance Magnitude Profile - Single Frequency Sinusoidal Modulation using the FFT Technique

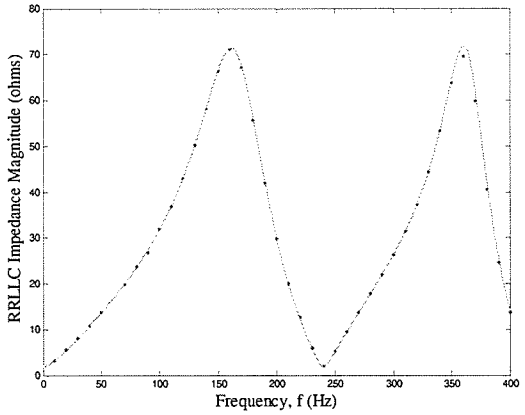

Figure 26: RRLLC Impedance Phase Profile - Single Frequency Sinusoidal Modulation using the FFT Technique

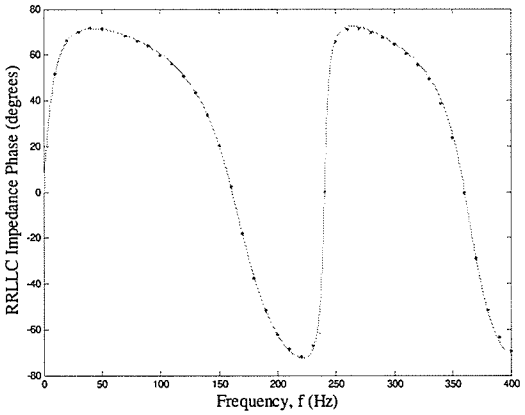

Figure 27: RRLLC Impedance Magnitude Profile - Multiple Frequency Sinusoidal Modulation using the FFT Technique

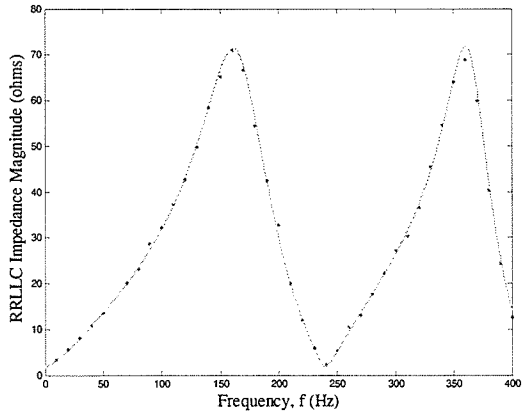

Figure 28: RRLLC Impedance Phase Profile - Multiple Frequency Sinusoidal Modulation using the FFT Technique

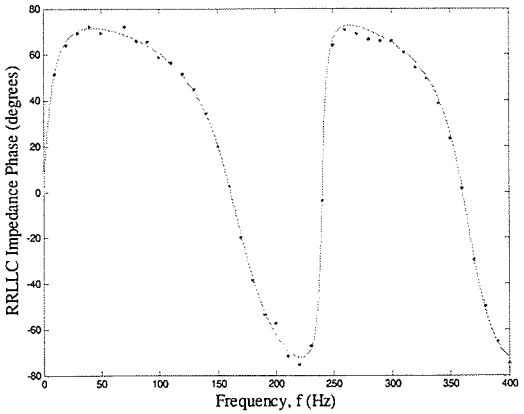

Figure 29: RRLLC Impedance Magnitude Profile - Multiple Frequency Sinusoidal Modulation using the DFT Technique

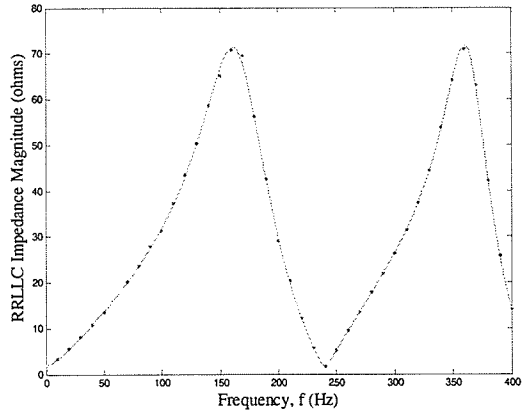

Figure 30: RRLLC Impedance Phase Profile – Multiple Frequency Sinusoidal Modulation using the DFT Technique

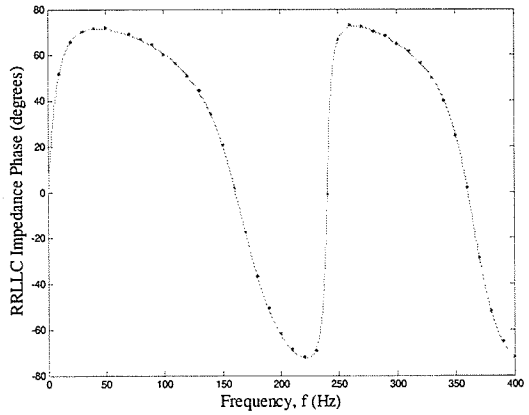

4.2.2 Summary of Simulation Results using the Simplified Model of a HVDC Link

The results of impedance profiling using the simplified model of a HVDC link indicate temporary firing angle modulation can be used to accurately profile RL, RRL, RLL and RRLLC impedance types. Accurate profiles were obtained after 2 or 3 seconds of modulation.

A single frequency modulation signal can be used to modulate the firing angle, have negligible effect on system operation and obtain an accurate impedance profile at specific frequencies. The AC network impedance profile can be accurately calculated over a wide frequency range by injecting many separate single frequency modulation signals, although such an undertaking is not practical in terms of time and effort.

Using multiple frequency modulation signals, accurate and rapid impedance profiling can be conducted over a wide frequency range without appreciably affecting the system operation by limiting the magnitude and phase staggering each sinusoidal component in the modulation signals.

The DFT method with high sampling frequency is superior to the FFT method with low sampling frequency. The FFT method was often inaccurate at frequencies near the fundamental frequency and at frequencies higher than five and a half times the fundamental frequency. Inaccuracies were sometimes evident at other frequencies. The DFT method is much more accurate in impedance profiling. Accurate impedance calculations were obtained at frequencies ranging from 10 Hz to 400 Hz.

4.3 Applying the Impedance Profiling Methods to the CIGRE HVDC Benchmark Model

CIGRE has established a benchmark model for HVDC studies. The model manifests many of the operating concerns of typical HVDC systems worldwide. This CIGRE model was used to further investigate the feasibility of impedance identification via inverter firing angle modulation. A schematic of the CIGRE benchmark model is shown in Figure 2 and a block diagram of the HVDC control system is given in Figure 3. The CIGRE model includes a detailed model of the HVDC rectifier, the HVDC inverter and the HVDC control system. In the model, the rated inverter AC bus bar voltage (RMS, line-line quantity) is 230 kV and the rated DC power of the HVDC link is 1000 MW. The impedance vector of the inverter filters (at the fundamental frequency of the AC system) has a value of $0.143 - 84.351j\ \Omega$. The inverter AC network impedance in the model was varied to represent a weak and a strong inverter AC network. The weak and strong network impedance models are shown in Figure 6. The weak network impedance model provides an additional impedance topology with which to test impedance profiling methods.

The impedance of the weak inverter network contains three resistors and two inductors. In the CIGRE benchmark model, resistor R_1 has a value of $0.7306\ \Omega$, R_2 has a value of $0.7406\ \Omega$ and R_3 has a value of $24.81\ \Omega$. Inductor L_1 and L_2 are set equal to 0.0365 H. Therefore, the weak inverter network has an impedance vector (at the fundamental frequency of the AC system) equal to $5.498 + 20.466j\ \Omega$. The SCR and ESCR were

defined in section 1.1. The SCR and ESCR of the weak network can be calculated as $2.496 \angle 74.96°$ S and $1.898 \angle 70.01°$ S respectively.

The impedance of the strong inverter network contains a 4.523 Ω resistive component and a 0.04 H inductive component. Therefore, the strong inverter network has an impedance vector (at the fundamental frequency of the AC system) equal to $4.523 + 12.566j\ \Omega$. The SCR and ESCR of the strong network can be calculated as $3.961 \angle 70.20°$ S and $3.378 \angle 66.58°$ S respectively.

To begin, the HVDC control system was removed from operation and the rectifier and inverter firing angle control signals were set to constant values. Although the HVDC control system could not be removed from operation in an actual operating power system, the control system can be removed in the CIGRE benchmark software model. Testing the impedance profiling methods with and without the HVDC control system in operation provides insight into the impact of the control system on impedance profiling. After the control system was removed from operation, a multiple frequency sinusoidal modulation signal was added to the inverter firing angle control signal. With the fundamental frequency of the AC system set at 50 Hz, positive sequence inverter AC network impedance profiles were calculated over the 5-400 Hz frequency band by injecting multiple frequency modulation signals with the following frequencies: 5, 10, 15, 20,..., 260 Hz and 270, 280, 290, 300,..., 350 Hz when using the FFT technique and 5, 10, 15, 20,..., 350 Hz when using the DFT technique. In each case, inverter firing angle modulation was conducted for 2 seconds. The multiple frequency

sinusoidal modulation signals were carefully chosen to produce detectable and measurable AC harmonics without causing noticeable disturbance on the AC system. The magnitude of each sinusoidal component in the modulation signals varies between $0.08°$ and $0.11°$. Each sinusoidal component was phase staggered – a phase staggering exponent of 3, 4 or 5 was used. This ensures no multiple frequency modulation signal has a magnitude exceeding $1.6°$. With a 20 μ s time step, AC network impedance identification was achieved using the FFT technique by first filtering the inverter AC bus bar voltage and current entering the inverter AC network. The fundamental frequency components and all frequency components outside the 5-1005 Hz frequency range were removed. The filtered voltage and current were passed through anti-aliasing filter and were continuously sampled. FFT analysis was carried out continuously over the 2 second modulation period. Also, the positive sequence component was extracted from each frequency component throughout the modulation period. The results given in section 4.3 for impedance identification using the FFT technique with the HVDC control system removed from operation are based on impedance profiles obtained near the end of the 2 second modulation period. With a 10 μ s time step, inverter AC network impedance identification was achieved using the DFT technique. The inverter AC bus bar voltage and current entering the inverter AC network were monitored throughout the 2 second modulation period. A 0.2 second portion of this voltage and current data (obtained near the end of the 2 second modulation period) was then input to the Matlab DFT program. This program performed DFT analysis on the voltage and current and then extracted the positive sequence component from each frequency component to calculate a positive sequence impedance profile of the inverter AC network.

Next, the HVDC control system was placed in operation. A multiple frequency sinusoidal modulation signal was added to the inverter firing angle control signal. As before, the fundamental frequency of the AC system was set at 50 Hz and positive sequence inverter AC network impedance profiles were calculated over the 5-400 Hz frequency band by injecting multiple frequency modulation signals with the following frequencies: 5, 10, 15, 20,..., 260 Hz and 270, 280, 290, 300,..., 350 Hz when using the FFT technique and 5, 10, 15, 20,..., 350 Hz when using the DFT technique.

The multiple frequency sinusoidal modulation signals were carefully chosen to produce detectable and measurable AC harmonics while limiting the interaction between the HVDC control system and the modulation signal and avoiding noticeable disturbance on the AC system. Injecting multiple frequency modulation signals with 5-350 Hz frequency ranges resulted in very large interactions between the HVDC control system and the modulation signal. These interactions caused wide variations in the inverter firing angle control signal and disturbed the AC system operation. Decreasing the magnitude of each sinusoidal component in the modulation signals did not substantially decrease the interactions. To limit the interactions, the frequency ranges of the multiple frequency modulation signals had to be decreased. For each inverter AC network impedance profile, three separate modulation signals were injected with the following frequency ranges: 5-150 Hz, 155-250 Hz and 255-350 Hz. When profiling a weak inverter AC network, the magnitude of each sinusoidal component in the modulation signals was chosen to be a small value (between $0.04°$ and $0.08°$) to avoid noticeable

disturbance on the AC system. When profiling a strong inverter AC network, the magnitude of each sinusoidal component in the modulation signals needed to be increased to obtain measurable harmonic voltages at the inverter AC bus bar. For a strong inverter AC network, the magnitude of each sinusoidal component varied between $0.08°$ and $0.20°$. Each sinusoidal component was phase staggered – a phase staggering exponent of 3, 4 or 5 was used. This ensured no multiple frequency modulation signal had a magnitude that exceeded $1.8°$. It also limited the variation in the inverter firing angle control signal to $4.9°$ and the variation in the rectifier firing angle control signal to $4.3°$.

Inverter firing angle modulation was conducted for 2 seconds. With a 20 μ s time step, AC network impedance identification was achieved using the FFT technique by first filtering the inverter AC bus bar voltage and current entering the inverter AC network. The fundamental frequency components and all frequency components outside the 5-1005 Hz frequency range were removed. The filtered voltage and current were passed through anti-aliasing filters and were continuously sampled. FFT analysis was carried out continuously over the 2 second modulation period. Also, the positive sequence component was extracted from each frequency component throughout the modulation period. The results given in section 4.3 for impedance identification using the FFT technique with the HVDC control system in operation are based on impedance profiles obtained near the end of the 2 second modulation period. With a 10 μ s time step, AC network impedance identification was achieved using the DFT technique. The inverter AC bus bar voltage and current entering the inverter AC network were monitored

throughout the 2 second modulation period. A 0.2 second portion of this voltage and current data (obtained near the end of the 2 second modulation period) was then input to the Matlab DFT program. This program performed DFT analysis on the voltage and current and then extracted the positive sequence component from each frequency component to calculate a positive sequence impedance profile of the inverter AC network.

All impedance profiles displayed in sections 4.3.1 and 4.3.2 are positive sequence impedance profiles. Also, the calculated impedance profile is always shown as a dotted line and the actual impedance profile is always shown as a solid line.

For all loading conditions and network strengths, adding multiple frequency sinusoidal modulation signals to the inverter firing angle control signal did not drastically disturb the AC system.

4.3.1 Testing the Impedance Profiling Methods under Various Loading Conditions

With the inverter AC network impedance modeled to represent a weak inverter AC network, the impedance profiling methods were tested under various DC line loading conditions by altering the DC current order. Impedance profiles were taken at unity current order, seventy percent current order and fifty percent current order.

It is important to test the impedance profiling methods at various DC current orders.

As the DC current order changes, a fixed modulation signal can cause different amounts of variation in the DC current magnitude. The system response to modulation varies as the DC current order is changed. In addition, the power demanded from an actual HVDC system varies from time to time and the desired power flow is achieved via the DC current order setting. Consequently, the DC current order will be varied during system operation.

4.3.1.1 Unity Current Order

With the HVDC control system removed from operation, the amplitude of the fundamental inverter AC bus bar voltage was modulated by a maximum of 7.2 kV (3.7% of the fundamental amplitude) and the amplitude of the fundamental current entering the inverter AC network was modulated by a maximum of 0.11 kA (3.1% of the fundamental amplitude).

The impedance profile obtained by completing inverter AC network impedance identification using the FFT technique is shown in Figure 31 and Figure 32. There are some inaccuracies in the calculated impedance profile at 350 Hz, 360 Hz, 390 Hz, 400 Hz and in the 240-310 Hz frequency range.

The impedance profile obtained by completing inverter AC network impedance identification using the DFT technique is shown in Figure 33 and Figure 34. Using

this technique, the calculated profile is very accurate over the 5-400 Hz frequency range, showing only minor error at 250 Hz, 310 Hz and above 340 Hz.

With the HVDC control system returned to normal operation, the amplitude of the fundamental inverter AC bus bar voltage was modulated by a maximum of 6.8 kV (3.5% of the fundamental amplitude) and the amplitude of the fundamental current entering the inverter AC network was modulated by a maximum of 0.22 kA (6.3% of the fundamental amplitude).

The impedance profile obtained by completing inverter AC network impedance identification using the FFT technique is shown in Figure 35 and Figure 36. There are some inaccuracies in the calculated impedance profile at 380 Hz, 400 Hz and in the 240-310 Hz frequency range.

The impedance profile obtained by completing inverter AC network impedance identification using the DFT technique is shown in Figure 37 and Figure 38. Using this technique, the calculated profile has some minor error at 295 Hz, 315 Hz, 320 Hz and in the 250-275 Hz frequency range. Larger error is present above 330 Hz. However, the profile calculated using the DFT technique is much more accurate than the profile calculated using the FFT technique.

Figure 31: Impedance Magnitude Profile of a Weak Inverter AC Network
at 1 P.U. DC Current - HVDC Control System Removed
From Operation and FFT Analysis

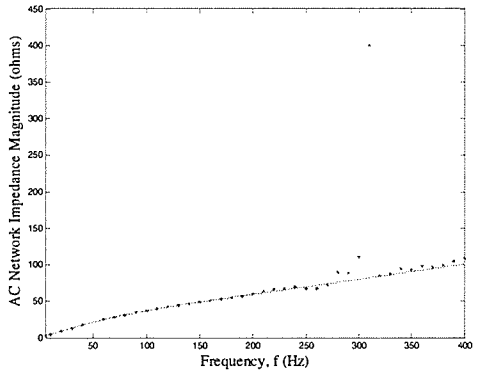

Figure 32: Impedance Phase Profile of a Weak Inverter AC Network
at 1 P.U. DC Current – HVDC Control System Removed
From Operation and FFT Analysis

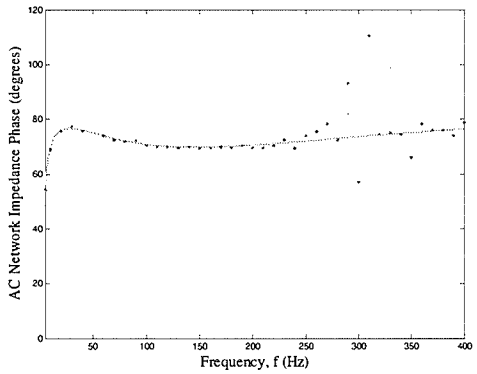

Figure 33: Impedance Magnitude Profile of a Weak Inverter AC Network
at 1 P.U. DC Current - HVDC Control System Removed
From Operation and DFT Analysis

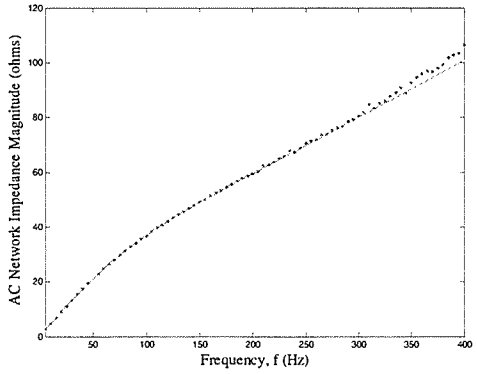

Figure 34: Impedance Phase Profile of a Weak Inverter AC Network
at 1 P.U. DC Current - HVDC Control System Removed
From Operation and DFT Analysis

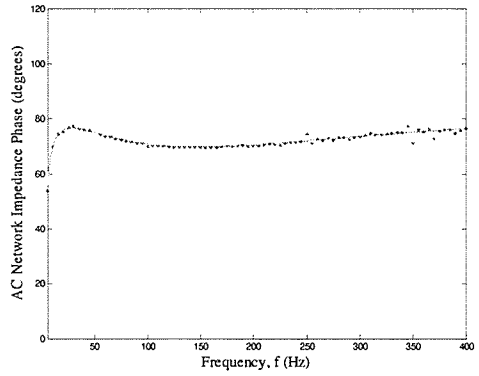

Figure 35: Impedance Magnitude Profile of a Weak Inverter AC Network
at 1 P.U. DC Current - HVDC Control System In Operation
and FFT Analysis

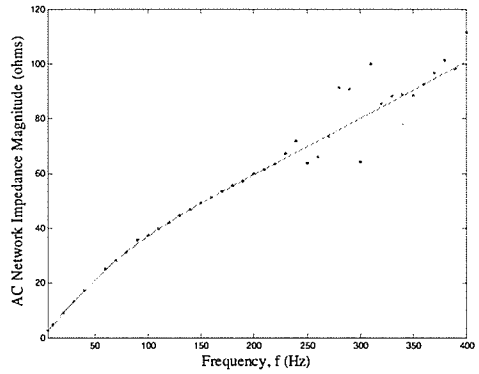

Figure 36: Impedance Phase Profile of a Weak Inverter AC Network
at 1 P.U. DC Current - HVDC Control System In Operation
and FFT Analysis

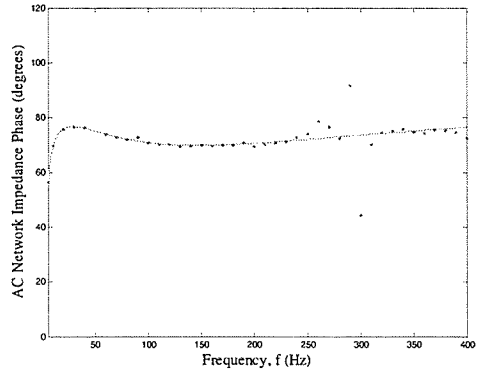

Figure 37: Impedance Magnitude Profile of a Weak Inverter AC Network
at 1 P.U. DC Current - HVDC Control System In Operation
and DFT Analysis

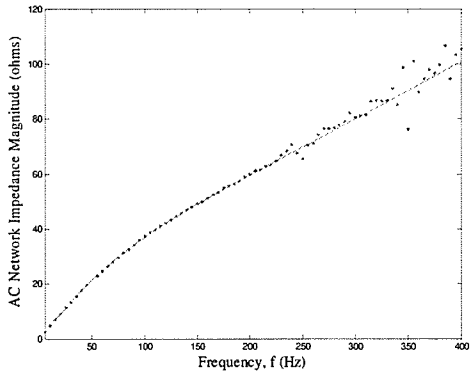

Figure 38: Impedance Phase Profile of a Weak Inverter AC Network
at 1 P.U. DC Current - HVDC Control System In Operation
and DFT Analysis

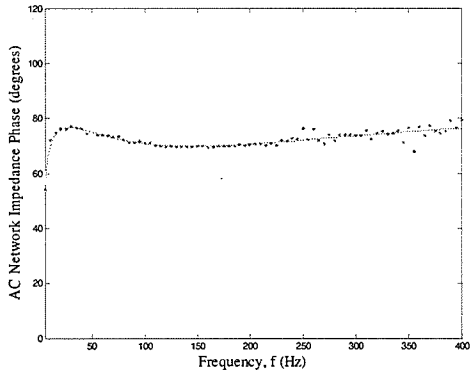

4.3.1.2 Seventy Percent Current Order

With the HVDC control system removed from operation, the amplitude of the fundamental inverter AC bus bar voltage was modulated by a maximum of 6.2 kV (2.9% of the fundamental amplitude) and the amplitude of the fundamental current entering the inverter AC network was modulated by a maximum of 0.09 kA (3.1% of the fundamental amplitude).

The impedance profile obtained by completing inverter AC network impedance identification using the FFT technique is shown in Figure 39 and Figure 40. There are some inaccuracies in the calculated impedance profile at 380 Hz, 400 Hz and in the 230-310 Hz frequency range.

The impedance profile obtained by completing inverter AC network impedance identification using the DFT technique is shown in Figure 41 and Figure 42. Using this technique, the calculated profile is very accurate over the 5-400 Hz frequency range, showing only minor error at 240 Hz.

With the HVDC control system returned to normal operation, the amplitude of the fundamental inverter AC bus bar voltage was modulated by a maximum of 4.4 kV (2.0% of the fundamental amplitude) and the amplitude of the fundamental current entering the inverter AC network was modulated by a maximum of 0.11 kA (3.8% of the fundamental amplitude).

The impedance profile obtained by completing inverter AC network impedance identification using the FFT technique is shown in Figure 43 and Figure 44. There are some inaccuracies in the calculated impedance profile at 380 Hz, 400 Hz and in the 250-300 Hz frequency range.

The impedance profile obtained by completing inverter AC network impedance identification using the DFT technique is shown in Figure 45 and Figure 46. Using this technique, the calculated profile is very accurate over the 5-400 Hz frequency range, showing only minor error at 100 Hz and 105 Hz.

Figure 39: Impedance Magnitude Profile of a Weak Inverter AC Network
at 0.7 P.U. DC Current - HVDC Control System Removed
From Operation and FFT Analysis

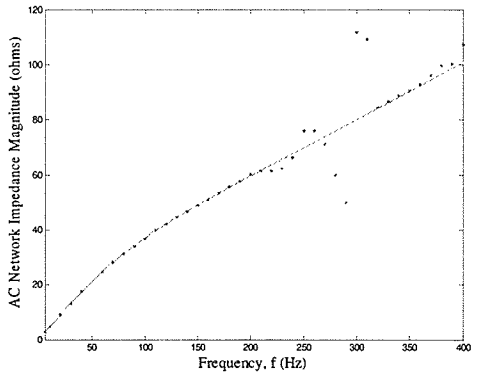

Figure 40: Impedance Phase Profile of a Weak Inverter AC Network
at 0.7 P.U. DC Current – HVDC Control System Removed
From Operation and FFT Analysis

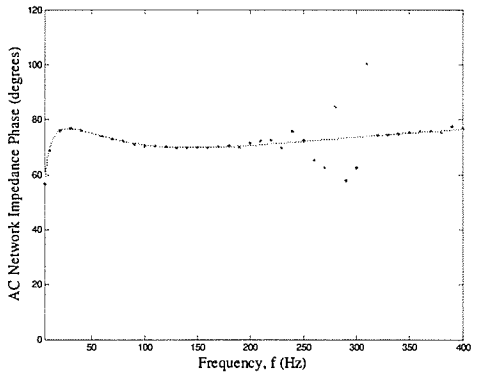

Figure 41: Impedance Magnitude Profile of a Weak Inverter AC Network
at 0.7 P.U. DC Current - HVDC Control System Removed
From Operation and DFT Analysis

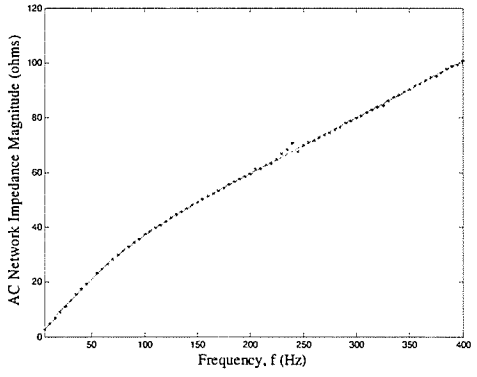

Figure 42: Impedance Phase Profile of a Weak Inverter AC Network
at 0.7 P.U. DC Current - HVDC Control System Removed
From Operation and DFT Analysis

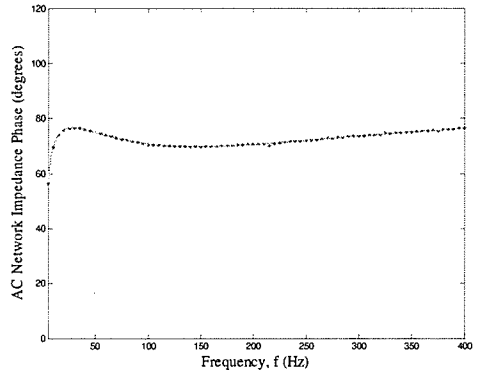

Figure 43: Impedance Magnitude Profile of a Weak Inverter AC Network
at 0.7 P.U. DC Current - HVDC Control System In Operation
and FFT Analysis

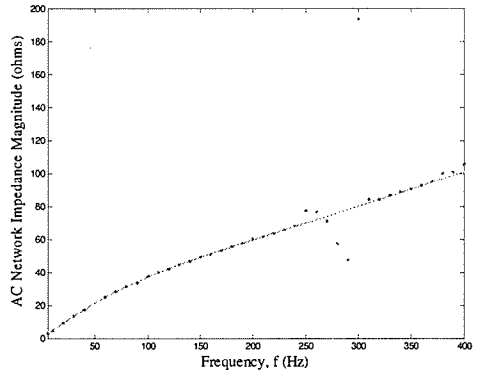

Figure 44: Impedance Phase Profile of a Weak Inverter AC Network
at 0.7 P.U. DC Current - HVDC Control System In Operation
and FFT Analysis

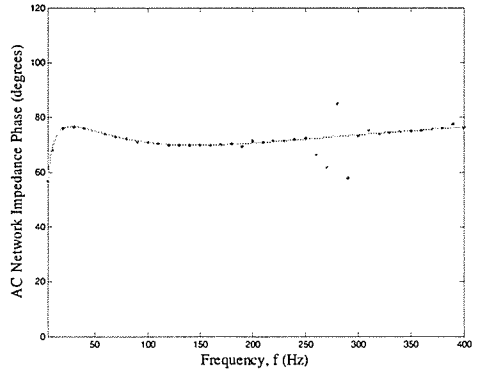

Figure 45: Impedance Magnitude Profile of a Weak Inverter AC Network
at 0.7 P.U. DC Current - HVDC Control System In Operation
and DFT Analysis

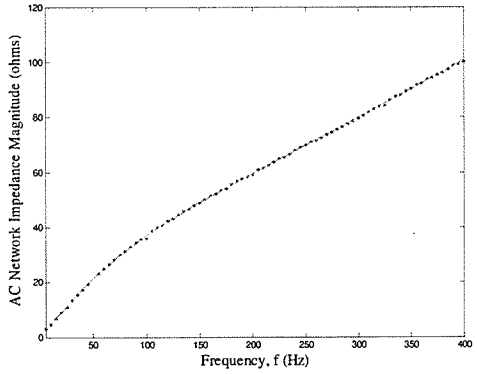

Figure 46: Impedance Phase Profile of a Weak Inverter AC Network
at 0.7 P.U. DC Current - HVDC Control System In Operation
and DFT Analysis

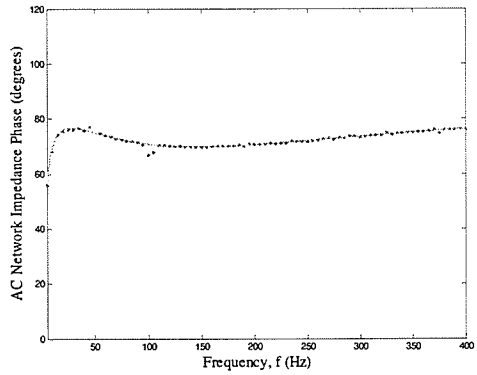

4.3.1.3 Fifty Percent Current Order

With the HVDC control system removed from operation, the amplitude of the fundamental inverter AC bus bar voltage was modulated by a maximum of 4.8 kV (2.1% of the fundamental amplitude) and the amplitude of the fundamental current entering the inverter AC network was modulated by a maximum of 0.12 kA (4.6% of the fundamental amplitude).

The impedance profile obtained by completing inverter AC network impedance identification using the FFT technique is shown in Figure 47 and Figure 48. There are some inaccuracies in the calculated impedance profile at 380 Hz, 400 Hz and in the 230-310 Hz frequency range.

The impedance profile obtained by completing inverter AC network impedance identification using the DFT technique is shown in Figure 49 and Figure 50. Using this technique, the calculated impedance profile is very accurate over the 5-400 Hz frequency range.

With the HVDC control system returned to normal operation, the amplitude of the fundamental inverter AC bus bar voltage was modulated by a maximum of 4.1 kV (1.8% of the fundamental amplitude) and the amplitude of the fundamental current entering the inverter AC network was modulated by a maximum of 0.08 kA (3.0% of the fundamental amplitude).

The impedance profile obtained by completing inverter AC network impedance identification using the FFT technique is shown in Figure 51 and Figure 52. There are some inaccuracies in the calculated impedance profile in the 250-310 Hz and 390-400 Hz frequency ranges.

The impedance profile obtained by completing inverter AC network impedance identification using the DFT technique is shown in Figure 53 and Figure 54. Using this technique, the calculated profile is very accurate over the 5-400 Hz frequency range, showing only minor error at 45 Hz, 315 Hz and 385 Hz.

Figure 47: Impedance Magnitude Profile of a Weak Inverter AC Network
at 0.5 P.U. DC Current - HVDC Control System Removed
From Operation and FFT Analysis

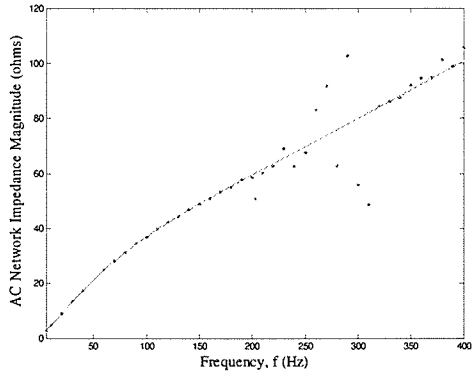

Figure 48: Impedance Phase Profile of a Weak Inverter AC Network
at 0.5 P.U. DC Current – HVDC Control System Removed
From Operation and FFT Analysis

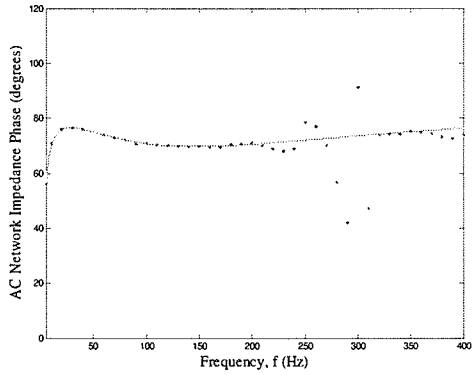

Figure 49: Impedance Magnitude Profile of a Weak Inverter AC Network
at 0.5 P.U. DC Current - HVDC Control System Removed
From Operation and DFT Analysis

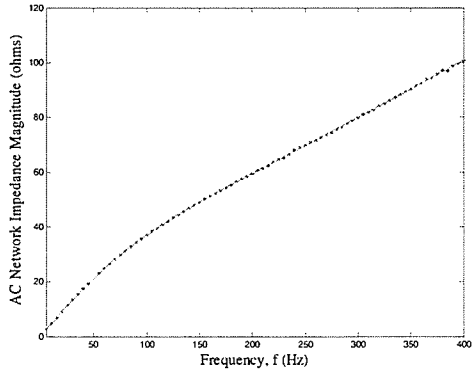

Figure 50: Impedance Phase Profile of a Weak Inverter AC Network
at 0.5 P.U. DC Current - HVDC Control System Removed
From Operation and DFT Analysis

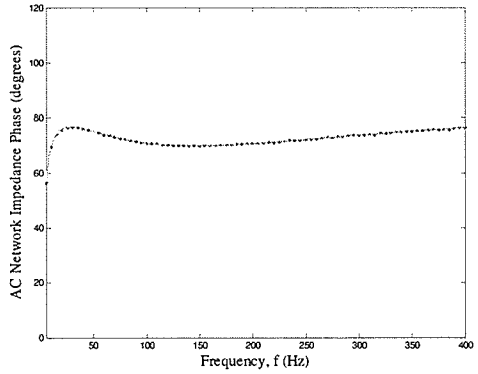

Figure 51: Impedance Magnitude Profile of a Weak Inverter AC Network
at 0.5 P.U. DC Current - HVDC Control System In Operation
and FFT Analysis

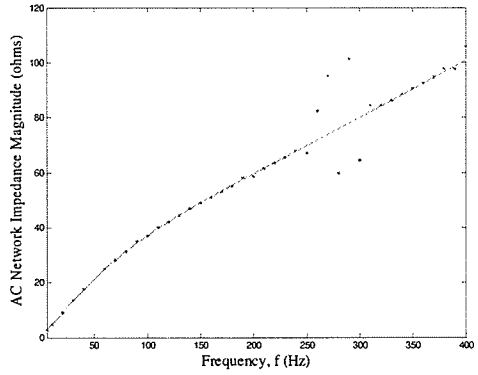

Figure 52: Impedance Phase Profile of a Weak Inverter AC Network
at 0.5 P.U. DC Current - HVDC Control System In Operation
and FFT Analysis

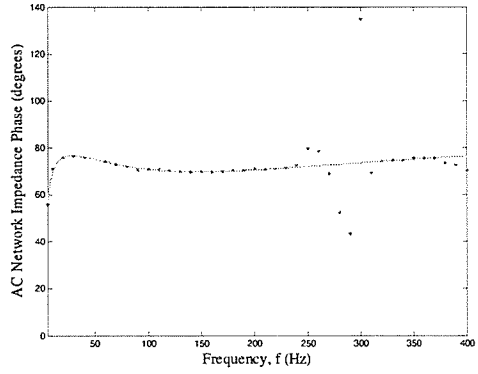

Figure 53: Impedance Magnitude Profile of a Weak Inverter AC Network
at 0.5 P.U. DC Current - HVDC Control System In Operation
and DFT Analysis

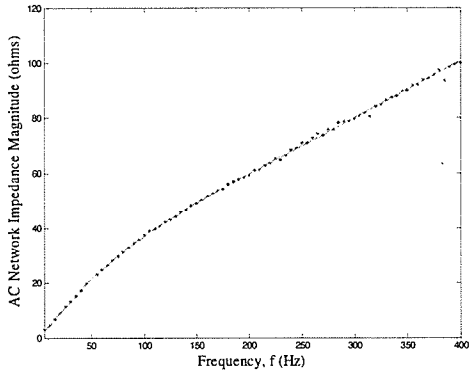

Figure 54: Impedance Phase Profile of a Weak Inverter AC Network
at 0.5 P.U. DC Current - HVDC Control System In Operation
and DFT Analysis

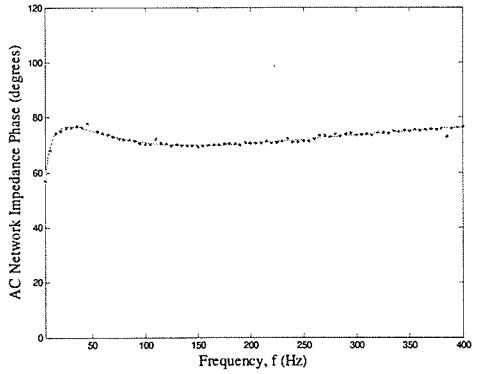

4.3.2 Testing the Impedance Profiling Methods with a Strong AC Network

The impedance profiling methods were next tested using a strong AC network (with the HVDC system operating at 1 P.U. DC current). It is important to test the impedance profiling methods with both strong and weak AC networks. When the AC network is weak, the commutating voltage may experience large variations. In contrast, when the AC network is strong, the commutating voltage does not vary greatly. The system response to a fixed modulation signal will vary as the strength of the AC network is changed. As the strength of the AC network is increased, it may be difficult to guarantee measurable harmonic voltages are generated at the AC bus bar without increasing the magnitude of each frequency component in the modulation signal.

With the HVDC control system removed from operation, the amplitude of the fundamental inverter AC bus bar voltage was modulated by a maximum of 7.6 kV (3.9% of the fundamental amplitude) and the amplitude of the fundamental current entering the inverter AC network was modulated by a maximum of 0.13 kA (3.7% of the fundamental amplitude).

The impedance profile obtained by completing inverter AC network impedance identification using the FFT technique is shown in Figure 55 and Figure 56. There are some inaccuracies in the calculated impedance profile at 340 Hz, 350 Hz, 390 Hz, 400 Hz and in the 240-310 Hz frequency range.

The impedance profile obtained by completing inverter AC network impedance identification using the DFT technique is shown in Figure 57 and Figure 58. Using this technique, the calculated profile is very accurate over the 5-400 Hz frequency range, showing only minor error at 345 Hz and 355 Hz.

With the HVDC control system returned to normal operation, the amplitude of the fundamental inverter AC bus bar voltage was modulated by a maximum of 10.4 kV (5.3% of the fundamental amplitude) and the amplitude of the fundamental current entering the inverter AC network was modulated by a maximum of 0.29 kA (8.2% of the fundamental amplitude).

The impedance profile obtained by completing inverter AC network impedance identification using the FFT technique is shown in Figure 59 and Figure 60. There are some inaccuracies in the calculated impedance profile at 400 Hz and in the 250-310 Hz frequency range.

The impedance profile obtained by completing inverter AC network impedance identification using the DFT technique is shown in Figure 61 and Figure 62. Using this technique, the calculated profile has some minor error at 150 Hz, 200 Hz, 310 Hz, 325 Hz and in the 250-275 Hz frequency range. Larger error is present in the 40-55 Hz, 95-105 Hz, 340-370 Hz and 385-400 Hz frequency ranges. However, the overall profile calculated using the DFT technique is more accurate than the overall profile calculated using the FFT technique.

Figure 55: Impedance Magnitude Profile of a Strong Inverter AC Network
at 1 P.U. DC Current - HVDC Control System Removed
From Operation and FFT Analysis

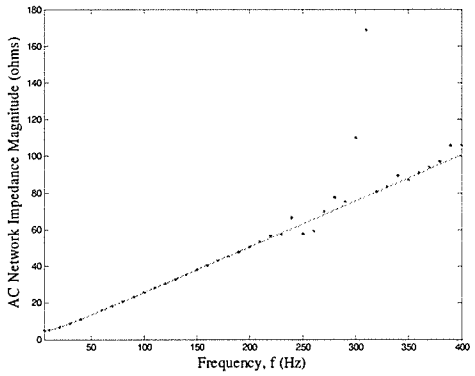

Figure 56: Impedance Phase Profile of a Strong Inverter AC Network
at 1 P.U. DC Current – HVDC Control System Removed
From Operation and FFT Analysis

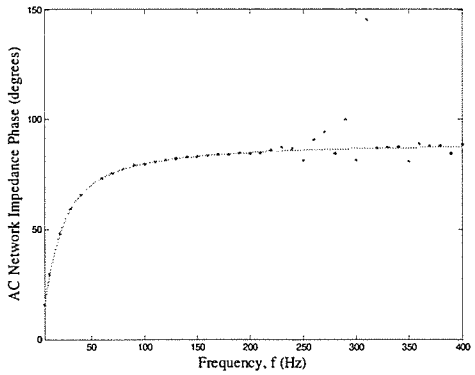

Figure 57: Impedance Magnitude Profile of a Strong Inverter AC Network
at 1 P.U. DC Current - HVDC Control System Removed
From Operation and DFT Analysis

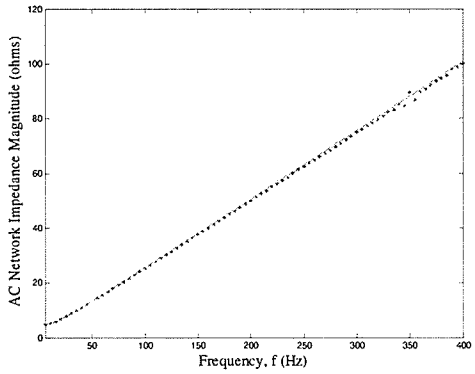

Figure 58: Impedance Phase Profile of a Strong Inverter AC Network
at 1 P.U. DC Current - HVDC Control System Removed
From Operation and DFT Analysis

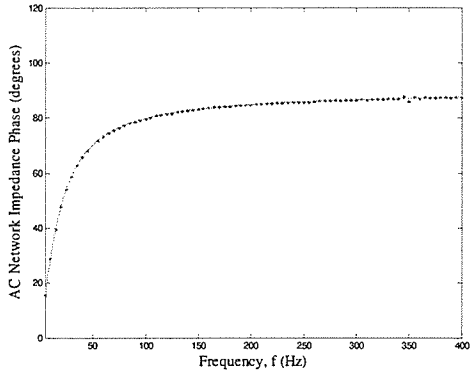

Figure 59: Impedance Magnitude Profile of a Strong Inverter AC Network
at 1 P.U. DC Current - HVDC Control System In Operation
and FFT Analysis

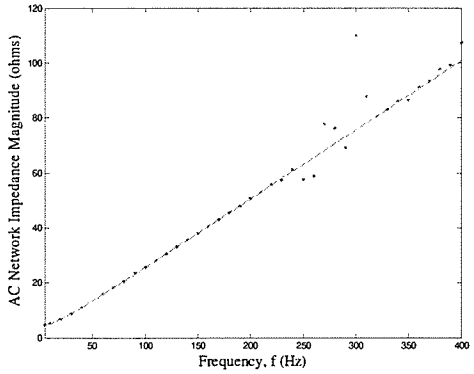

Figure 60: Impedance Phase Profile of a Strong Inverter AC Network
at 1 P.U. DC Current - HVDC Control System In Operation
and FFT Analysis

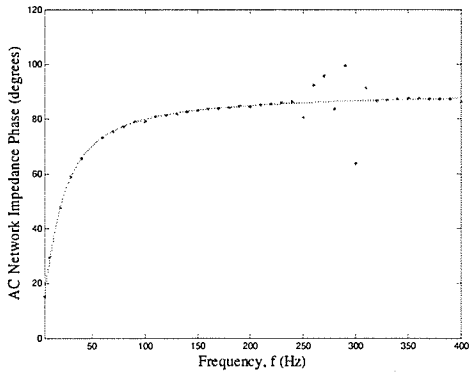

Figure 61: Impedance Magnitude Profile of a Strong Inverter AC Network
at 1 P.U. DC Current - HVDC Control System In Operation
and DFT Analysis

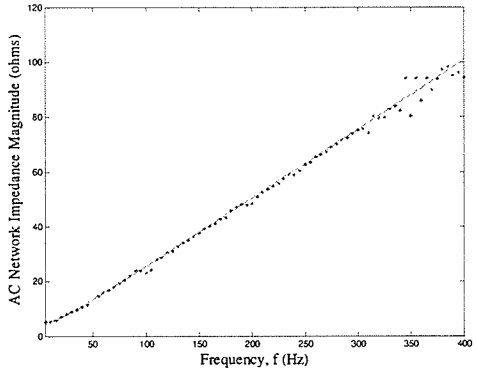

Figure 62: Impedance Phase Profile of a Strong Inverter AC Network
at 1 P.U. DC Current - HVDC Control System In Operation
and DFT Analysis

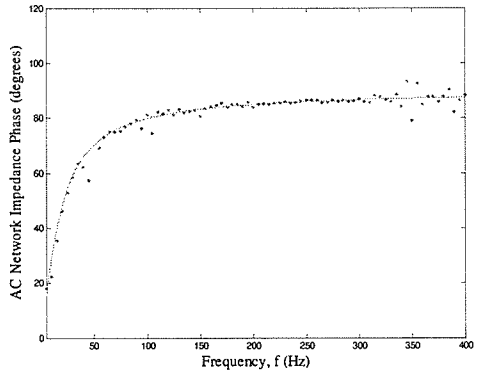

4.3.3 Testing the DFT Impedance Profiling Method with Various Durations of Modulation

As previously mentioned, all the results given in sections 4.3.1 and 4.3.2 were obtained using a 2 second modulation period. It is important to determine the effect of modulation duration on the accuracy of the calculated impedance profile. When implementing an impedance profiling method on an operating power system, the modulation duration

could be shortened as much as is possible without substantially degrading the accuracy of the calculated impedance profile. This would increase the speed of impedance identification.

Using a weak AC network, with an operating HVDC control system and 0.5 P.U. DC current, the DFT impedance identification technique was used to obtain AC network impedance profiles after varying durations of modulation. Figure 63 shows the effect of modulation duration on the accuracy of the calculated AC network impedance magnitude. The RMS error in the impedance magnitude calculation, over the 5-400 Hz frequency range, is plotted versus modulation duration.

Figure 63: RMS Error in the Impedance Magnitude Calculation over the 5-400 Hz Frequency Range - HVDC Control System In Operation, 0.5 P.U. DC Current and DFT Analysis

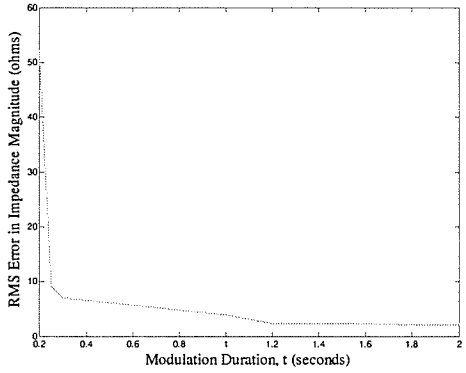

It is evident that the firing angle should be modulated for a minimum of 1.2 seconds. Shortening the modulation duration to less than 1.2 seconds results in a substantial increase in error in the calculated impedance profile.

4.3.4 Summary of Simulation Results using the CIGRE HVDC Benchmark Model

Simulations using the CIGRE benchmark model of a HVDC link demonstrate that temporary multiple frequency inverter firing angle modulation can be used to accurately profile inverter AC network impedances over a range of system conditions and operating points. In general, decreasing the DC current order improves the accuracy of the calculated impedance profile. When the system has a strong inverter AC network, the magnitude of the modulation must often be increased to obtain measurable harmonic voltages at the inverter AC bus bar. When the system has a weak inverter AC network, the modulation magnitude must often be decreased to avoid affecting system operation.

Although the HVDC control system could not be removed from operation in an actual operating power system, the control system can be removed in the CIGRE benchmark software model. With the HVDC control system removed from operation, accurate and rapid impedance profiling can be conducted over a wide frequency range without appreciably affecting the system operation by limiting the magnitude and phase staggering each sinusoidal component in the modulation signals. With the HVDC control system in operation, interactions between the control system and the modulation signals can affect the accuracy the calculated impedance profiles. However, acceptable impedance profiles can be obtained by limiting the frequency range and magnitude of the

modulation signals and phase staggering each sinusoidal component in the modulation signals.

The DFT method with high sampling frequency is superior to the FFT method with low sampling frequency. The FFT method was often inaccurate at frequencies around five and a half times the fundamental frequency and at frequencies higher than seven and a half times the fundamental frequency. The DFT method was often quite accurate in impedance profiling. After 2 seconds of modulation, accurate impedance calculations were obtained at frequencies ranging from 5 Hz to 400 Hz. Examination of the RMS error in the impedance magnitude calculations suggests that the firing angle should be modulated for a minimum of 1.2 seconds to obtain accurate impedance calculations.

Chapter 5: Ride-through Capability of a HVDC Link During Firing Angle Modulation

The results from Chapter 4 indicate that temporary multiple frequency inverter firing angle modulation can be used to accurately profile inverter AC network impedances over a range of system conditions and operating points. Accurate profiles can be obtained after 2 or 3 seconds of modulation, assuming there are no significant system transients or disturbances during this period.

The occurrence of some significant system disturbances, such as AC and DC line faults, cannot be predicted. It is possible that these disturbances could occur while modulating the inverter firing angle signal and could affect the calculated impedance profile. The error in the calculated impedance profile is not a significant concern, as the impedance profile could easily be recalculated after the power system returns to steady state operation. However, one concern is the effect of firing angle modulation on system recovery from these disturbances. The firing angle modulation signal should not affect the system recovery. To ensure the feasibility of measuring the inverter AC network impedance via modulation of the inverter firing angle signal while the network impedance is connected to the power system, the ride-through capability of a HVDC link with a modulated firing angle must be verified.

Verification of the ride-through capability was completed using the International Council on Large Electric Systems (CIGRE) benchmark model (Figure 2) with the HVDC control system (Figure 3) in operation. A weak inverter AC network was used, with a 1 P.U. DC steady state current.

Many system transients and disturbances were considered, including a 10% increase or decrease in DC current order, an AC single line to ground (SLG) fault at the inverter and a DC line fault. Each system transient or disturbance occurred at 0.3 seconds. For each system transient and disturbance, tests were completed using multiple frequency modulation signals with the following frequency ranges: 5-150 Hz, 155-250 Hz and 255-350 Hz. The modulation signals were added to the inverter firing angle control signal from 0.2 seconds to 1.2 seconds. The magnitude of each sinusoidal component in the modulation signals varied between $0.04°$ and $0.08°$. Each sinusoidal component was phase staggered – a phase staggering exponent of 3, 4 or 5 was used.

For each system transient and disturbance, system performance remained similar when a 5-150 Hz, 155-250 Hz or 255-350 Hz frequency range modulation signal was added to the inverter firing angle control signal. The figures displayed in sections 5.1-5.3 show various voltages, currents and control signals when the inverter firing angle control signal is not modulated and when a 5-150 Hz frequency range modulation signal is added to the inverter firing angle control signal.

5.1 Current Order Change

The power demanded from a HVDC link may vary from time to time. A change in power is obtained via an appropriate change in the DC current order input to the firing angle control system. For this reason a change in the DC current order is an expected system transient that could occur during firing angle modulation. Hence, an increase and decrease in DC current order were considered in verifying the ride-through capability of a HVDC link during firing angle modulation.

First, the DC current order was increased from 1 P.U. to 1.1 P.U. at 0.3 seconds. The resulting system voltages, currents and control signals are displayed in Figure 63 and Figure 64. It is evident that the modulation signal does not significantly affect system performance following the current order increase. The inverter AC bus bar and DC voltages decrease after 0.3 seconds.

Figure 64: System Response to a 0.1 P.U. DC Current Order Increase – No Firing Angle Control Signal Modulation

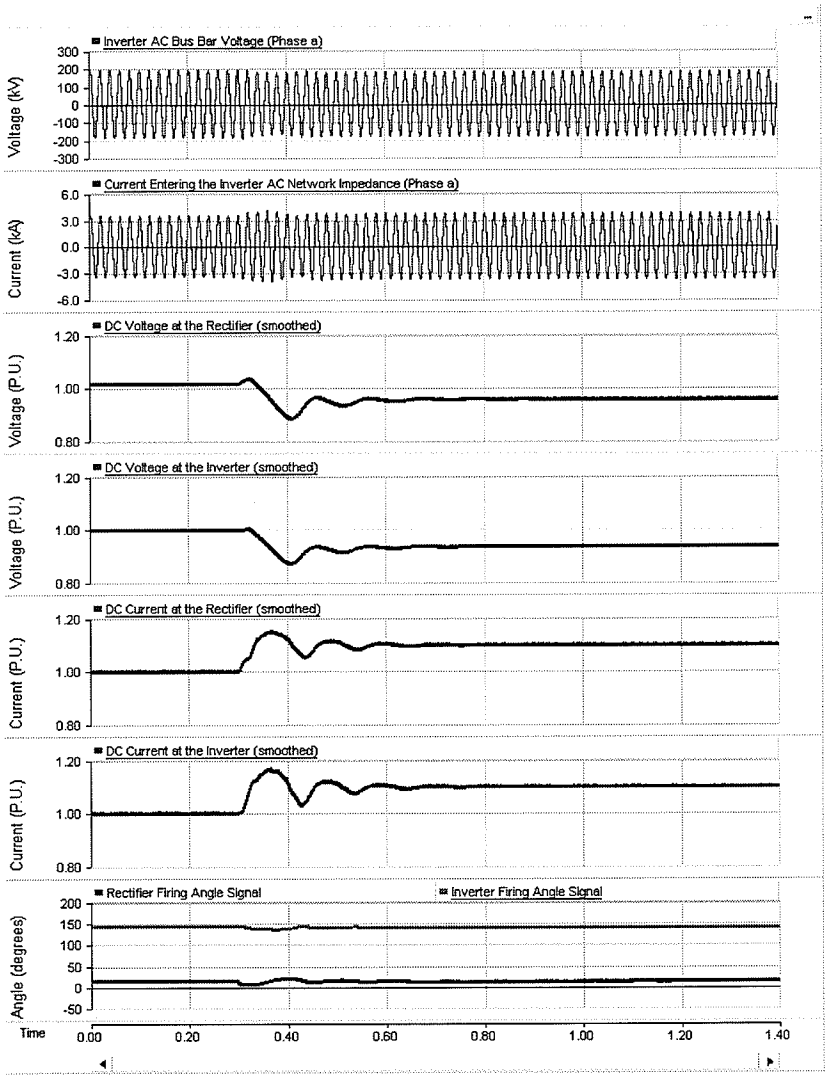

Figure 65: System Response to a 0.1 P.U. DC Current Order Increase – 5-150 Hz Frequency Range Modulation Signal

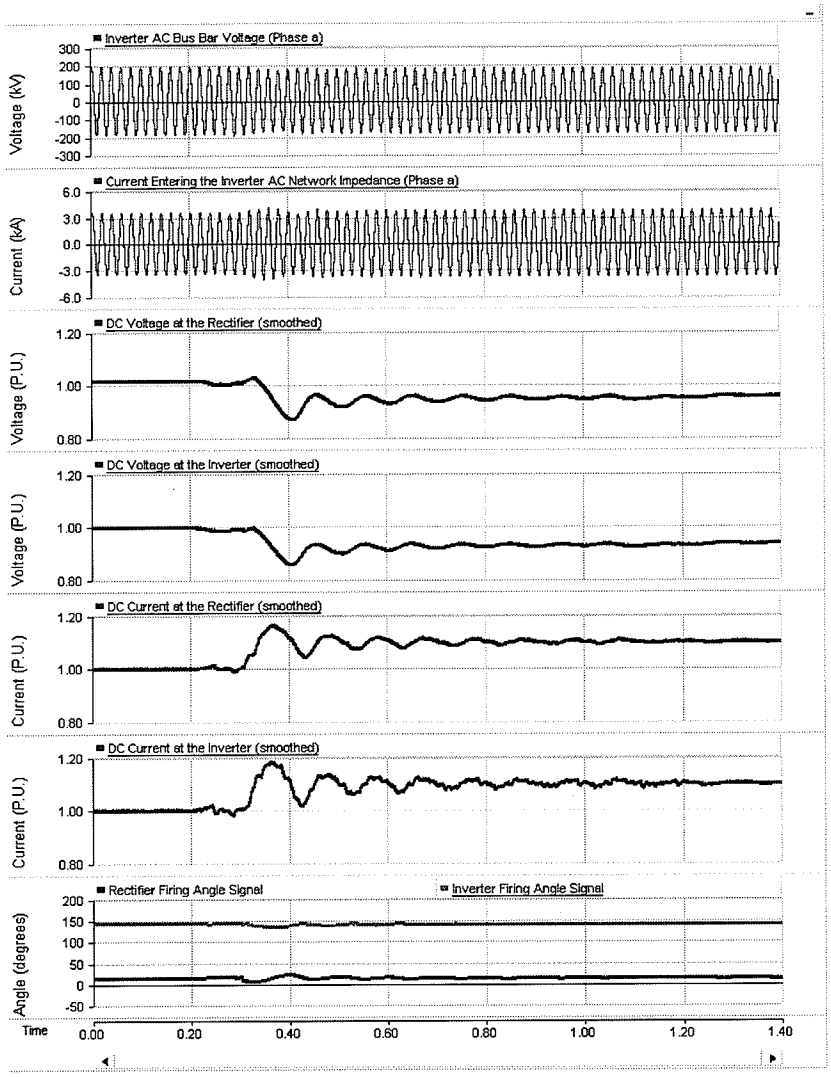

Next, the DC current order was decreased from 1 P.U. to 0.9 P.U. at 0.3 seconds. The resulting system voltages, currents and control signals are displayed in Figure 65 and Figure 66. The modulation signal does not significantly affect system performance following the current order decrease. The inverter AC bus bar and DC voltages increase after 0.3 seconds.

Figure 66: System Response to a 0.1 P.U. DC Current Order Decrease – No Firing Angle Control Signal Modulation

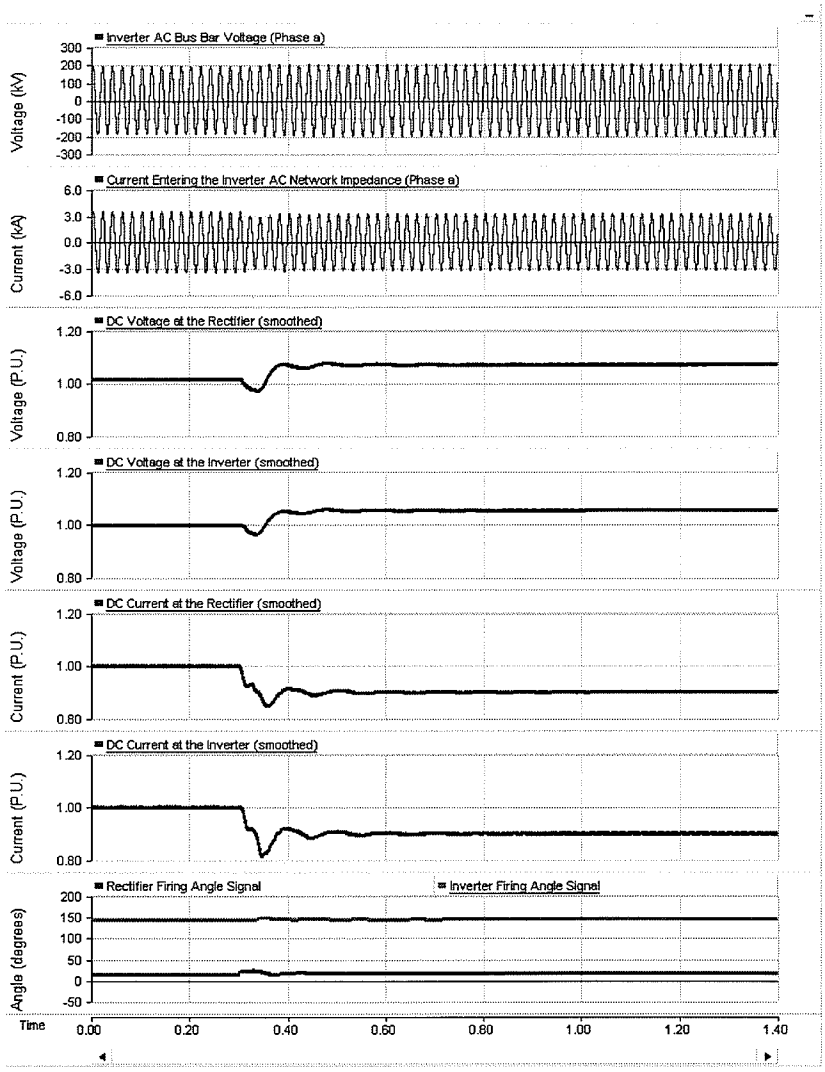

Figure 67: System Response to a 0.1 P.U. DC Current Order Decrease - 5-150 Hz Frequency Range Modulation Signal

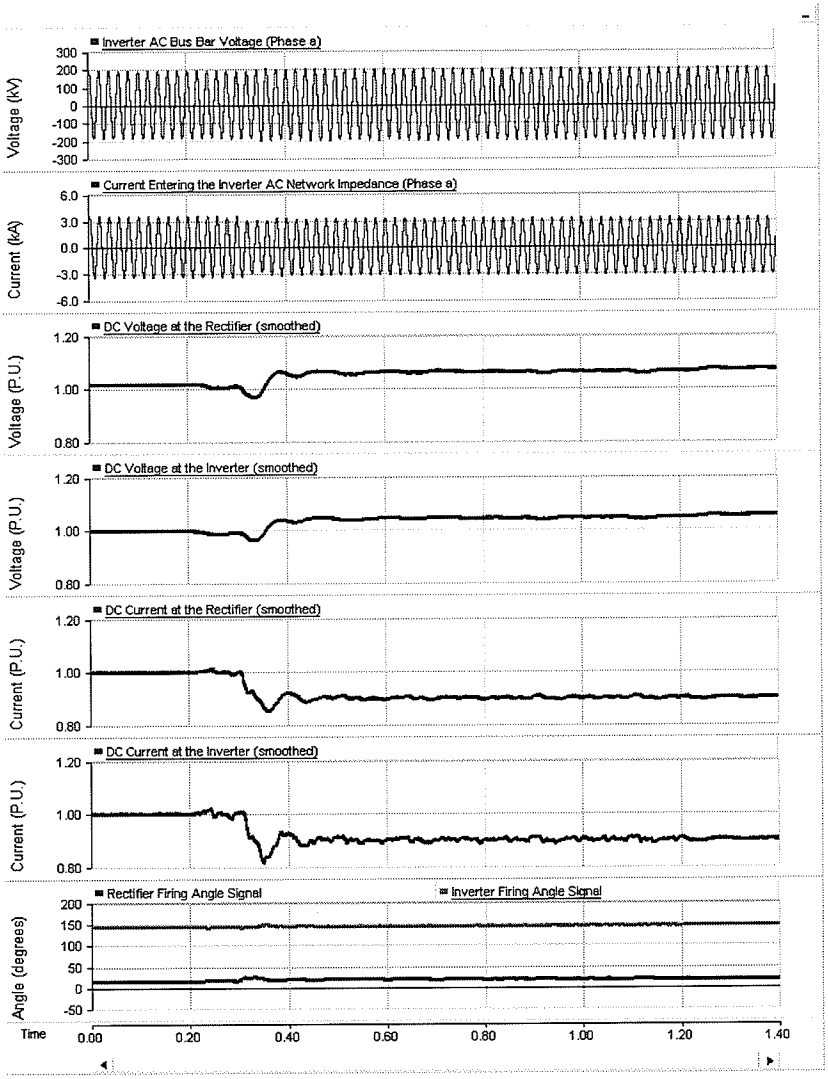

5.2 DC Line Fault

The next set of verification tests involved a DC line fault. Unlike AC line faults, DC line faults cannot be cleared by breaker operation because there is no natural zero crossing of DC current that would enable a breaker to open. Hence, DC line faults are cleared via a DC fault recovery protection sequence. After a DC line fault occurs, the fault recovery protection sequence is designed to transiently ramp up the rectifier firing angle control signal to 150° for 0.15 seconds. This rapidly removes energy from the fault and forces it out to the AC systems at the rectifier and inverter.

A DC line fault was applied at 0.3 seconds and was 0.05 seconds in duration. The resulting system voltages, currents and control signals are displayed in Figure 67 and Figure 68. The modulation signal does not significantly affect system recovery following the line fault. The DC voltages drop quite low during the fault. The fault is cleared after the DC current drops to zero due to the fault recovery protection sequence. Once the fault is cleared, the DC current and voltages recover to 90% of their pre-disturbance values by 0.56 seconds. Hence, the interruption of power from the HVDC link is limited to approximately 0.26 seconds.

Figure 68: System Response to a DC Line Fault – No Firing Angle Control Signal Modulation

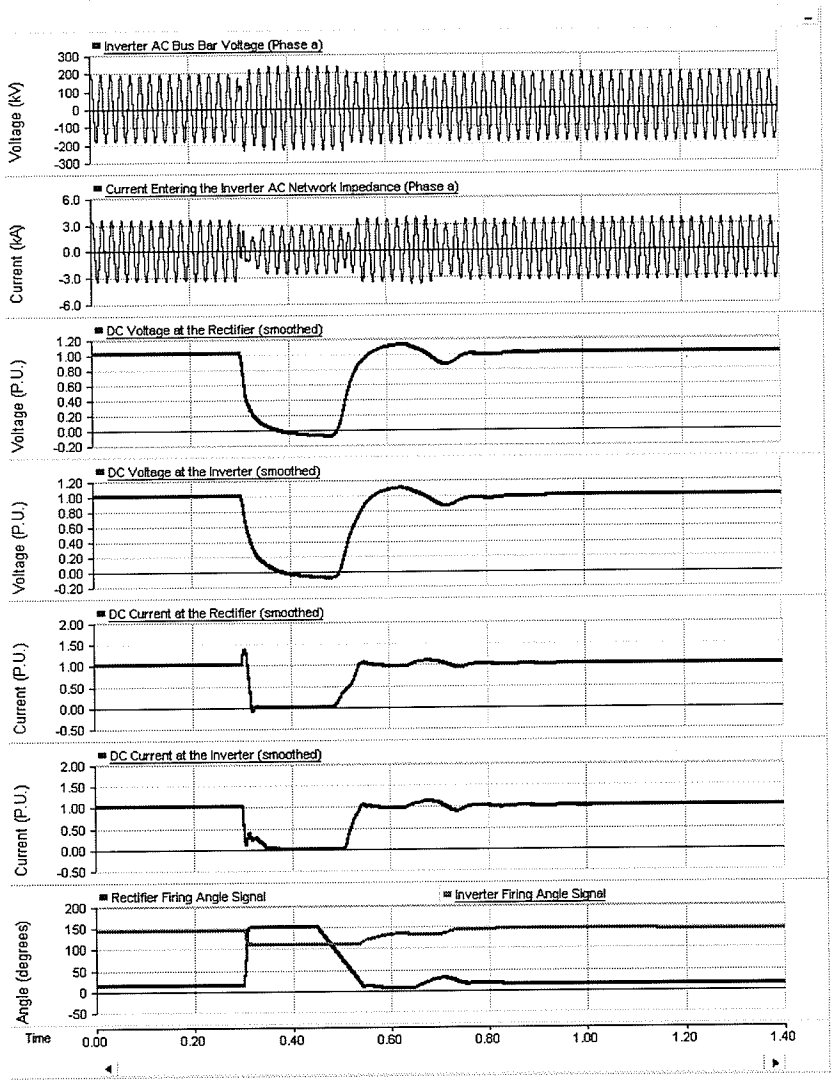

Figure 69: System Response to a DC Line Fault - 5-150 Hz Frequency Range Modulation Signal

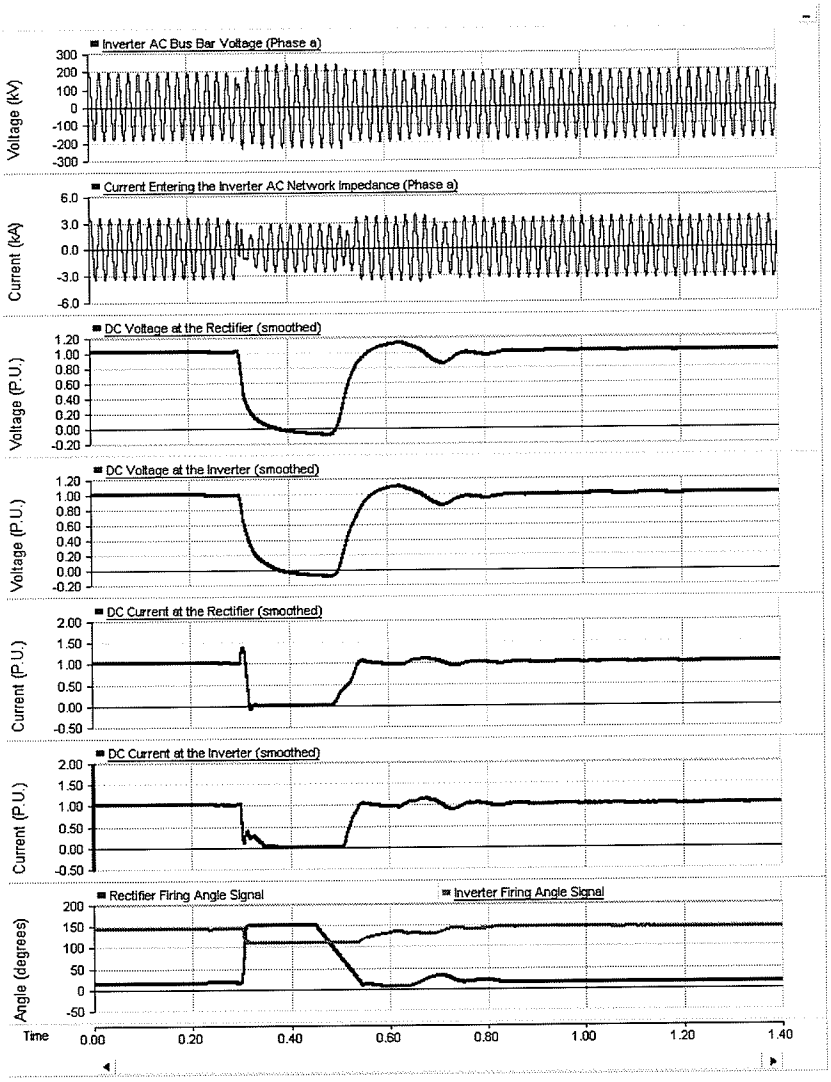

5.3 Single Line to Ground Fault at the Inverter AC Bus Bar

The most common AC line fault is a single line to ground (SLG) fault. Hence, it is important to verify the ride-through capability of a HVDC link during firing angle modulation when a SLG fault occurs.

A 5 cycle, phase a SLG fault was applied at the inverter AC bus bar at 0.3 seconds and was 0.1 seconds in duration. The resulting system voltages, currents and control signals are displayed in Figure 69 and Figure 70. The modulation signal does not significantly affect system recovery following the SLG fault at the inverter AC bus bar. When the fault occurs, the rectifier firing angle control signal temporarily increases to 150° in an attempt to limit the DC current at the rectifier. As a result, the DC current and voltages drop quite low. After the fault is cleared, the DC current and voltages begin to increase and recover to 90% of their pre-disturbance values by 0.54 seconds. Hence, the interruption of power from the HVDC link is limited to approximately 0.24 seconds.

Figure 70: System Response to a SLG Fault at the Inverter AC Bus Bar – No Firing Angle Control Signal Modulation

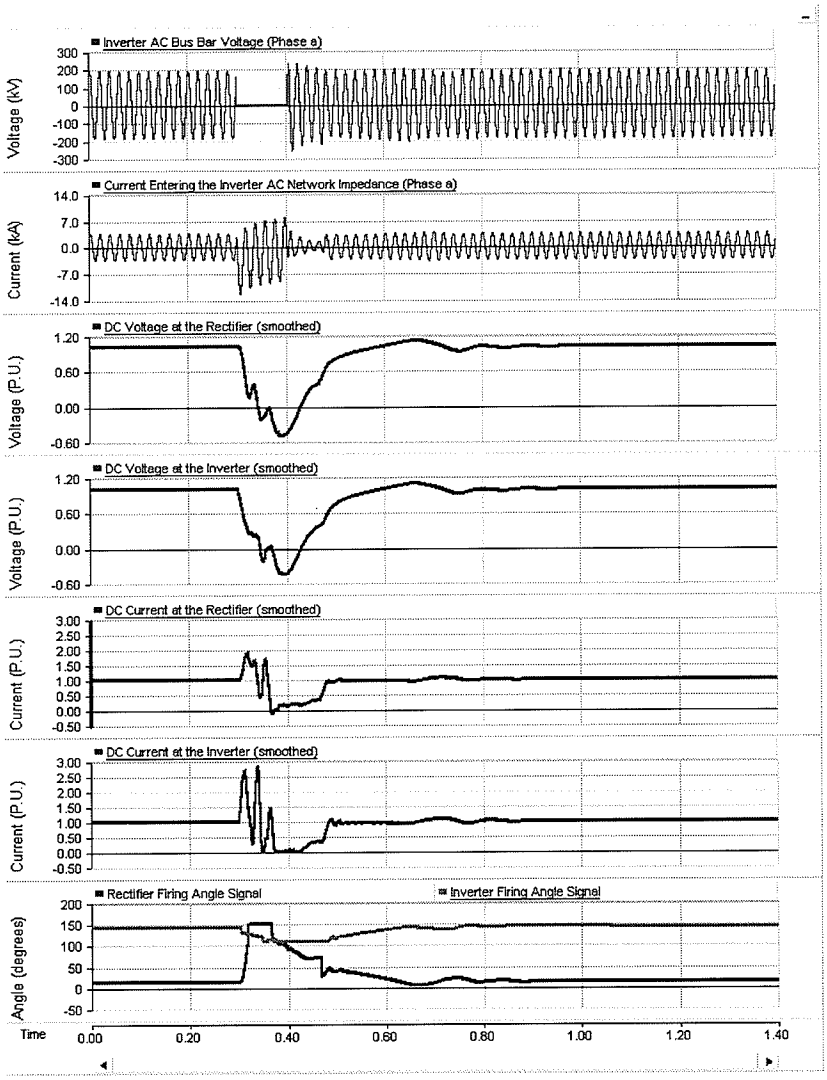

Figure 71: System Response to a SLG Fault at the Inverter AC Bus Bar - 5-150 Hz Frequency Range Modulation Signal

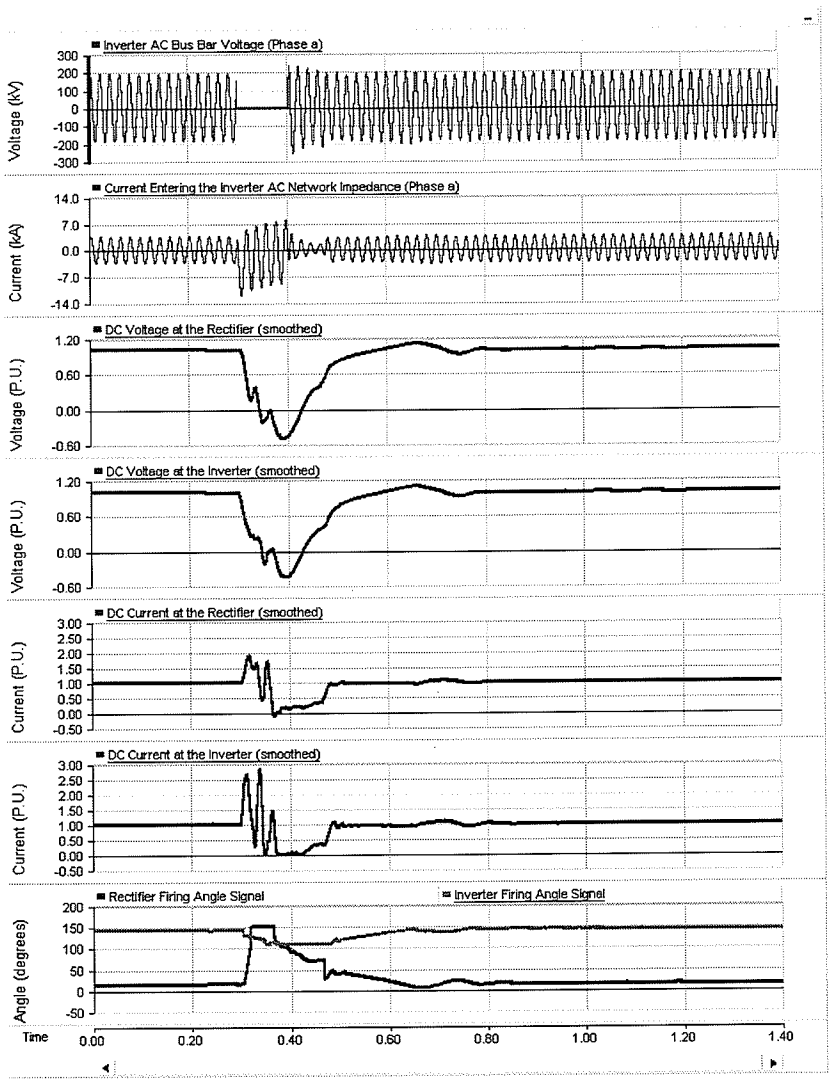

5.4 Summary of Ride-Through Capability Investigation Results

Exhaustive testing was carried out to verify the ride-through capability of a HVDC link during firing angle modulation. The modulation did not significantly affect power system operation or recovery from expected system transients or disturbances. A HVDC link with a modulated firing angle has ride-through capability for a change in DC current order, an AC SLG fault and a DC line fault. Therefore, it is feasible to modulate the converter's firing angle control signal while the power system is in operation. Modulation need not be stopped when a system transient or disturbance is detected. This does not mean impedance profile calculations will be accurate during transients and disturbances. If a transient or disturbance occurs while measuring the AC network impedance, the accuracy of the calculated impedance profile may be compromised. Impedance profiles should be calculated when the power system is in steady state operation.

Chapter 6: Contributions, Conclusions and Recommendations

The purpose of this thesis was to develop a method to accurately determine the AC network impedance characteristics at a HVDC link. More specifically, the goal was to develop a technique that can be used to determine the impedance profile of such an AC network over a frequency range without disturbing system operation.

There are many motivating reasons driving the development of a feasible AC network impedance profiling technique. Knowledge of the characteristics of the AC network impedance at a HVDC link is of vital importance to the operation of the HVDC link. In addition, knowledge of the AC network impedance profile can allow for the optimization of system performance. One could implement protection, damping and control systems that are dependent on the existing network impedance profile. Finally, network resonances could be resolved and existing models of the network impedance could be verified and enhanced.

6.1 Contributions and Conclusions

The thesis research focused on investigating and developing a method to accurately determine the AC network impedance characteristics at a HVDC link. Many conclusions can be drawn from the research completed for this thesis. The major contributions and conclusions are discussed below.

6.1.1 Theory of AC Network Impedance Profiling via Firing Angle Modulation

The theory behind impedance profiling via firing angle modulation was investigated using simple mathematical analysis of a HVDC link. Specifically, single frequency modulation of the firing angle control signal was considered. The analysis demonstrates that AC network impedance profiling via modulation of the firing angle signal is theoretically possible. In addition, results of the analysis provide insight to system behavior during multiple frequency sinusoidal modulation, provided the modulation does not cause a significant system disturbance.

6.1.2 Feasibility of AC Network Impedance Profiling via Firing Angle Modulation

The impedance profile of an AC network at a HVDC link can be calculated by measuring the current entering the AC network and the voltage of the AC bus bar while modulating the firing angle signal. The AC network impedance at the HVDC rectifier can be identified via modulation of the rectifier's firing angle signal. Similarly, the AC network impedance at the HVDC inverter can be identified via modulation of the inverter's firing

angle signal. Accurate profiles can be obtained after 1.2 seconds of modulation, assuming there are no significant system transients or disturbances during this period.

Impedance profiling via the firing angle modulation technique should not be attempted during a significant system transient or disturbance. If a transient or disturbance occurs while measuring the AC network impedance, the accuracy of the calculated impedance profile may be compromised.

Identifying the impedance profile of the AC network over a frequency range provides more information than that provided by the Short Circuit Ratio (SCR) and Effective Short Circuit Ratio (ESCR) of the AC system. These ratios are calculated only at the fundamental frequency of the AC system. Consequently, these ratios do not accurately reflect the transient behavior of the AC network impedance.

6.1.3 Ride-through Capability of a HVDC Link During Firing Angle Modulation

The ride-through capability of a HVDC link with a modulated firing angle was verified to ensure the feasibility of modulating the converter's firing angle control signal while the power system is in operation. Firing angle modulation does not negatively affect system performance or recovery following an AC single line to ground (SLG) fault, a DC line fault or a change in DC current order. Therefore, AC network impedance measurement can be carried out while the impedance is connected to the operating power system. This is a major advantage of AC network impedance profiling via modulation of the firing

angle signal. The modulation signal is added to the firing angle control signal while the power system is in operation.

6.1.4 Optimum Choice of Modulation Signal

Many possible modulation signals were investigated to determine the most practical choice of modulation signal. Single frequency modulation is not practical when determining the AC network impedance profile over a wide frequency range, as it involves injecting a huge number of separate firing angle modulation signals. Such an undertaking is not practical in terms of time and effort. The drawback to white noise modulation is the likelihood of disturbing system operation. When white noise is injected, it is not possible to control the frequency range or magnitude of the AC harmonics that are produced. Although one may be interested in the AC network impedance over a distinct frequency band, the range of produced harmonics on the AC system will likely be much larger than this band making it extremely difficult to detect and accurately measure the current through and voltage across the AC network impedance over the frequency band of interest. Multiple frequency modulation is the best choice of modulation signal. Using this type of modulation signal, it is possible to quickly generate an accurate impedance profile over a wide frequency band.

6.1.5 Modulation Signal Construction

Obtaining an accurate impedance profile via multiple frequency modulation requires careful construction of the modulation signal. Each frequency component in the modulation signal must be large enough to generate measurable voltages and currents on the AC network. At the same time, the modulation must not disturb or significantly affect system operation. To decrease the overall magnitude of the modulation signal and minimize the bunching effect discussed in section 3.1.2.1, the phase of each frequency component in the signal should be staggered. Also, the number of modulation frequencies should be limited to avoid large interactions between the HVDC control system and modulation signal. A low interaction was achieved when as many as 30 frequencies were included in the modulation signal. Superposition is valid when the multiple frequency modulation does not cause a significant system disturbance. When the AC network impedance is of interest over a specific frequency band, one can use superposition to determine the required modulating frequencies. A υ modulating frequency produces a significant positive sequence voltage and current on the AC system at frequency ($\upsilon + f_o$) and a significant negative sequence voltage and current on the AC system at frequency ($\upsilon - f_o$).

6.1.6 Impedance Profile Calculation

To calculate the impedance profile of an AC network at a HVDC link, the current entering the AC network and the voltage of the AC bus bar must be measured while modulating the firing angle signal. The fundamental frequency components present in the measured AC signals can be removed prior to harmonic analysis of these signals. This increases the signal to noise ratio (SNR) of the measured AC signals and increases the accuracy of the calculated impedance profile. Also, when impedance profiling over a specific frequency range, the SNR of the measured AC signals can be improved by effectively eliminating all frequency components outside the frequency range of interest. Two methods were used to calculate the harmonic components in the measured current and voltage – a Fast Fourier Transform (FFT) method with low sampling frequency and a Discrete Fourier Transform (DFT) method with high sampling frequency. With the FFT method, harmonic components are immediately calculated. With the DFT method, a finite amount of time is required to decompose the measured voltage and current into their harmonic components. Once the harmonic components are known, each component must then be broken down into sequence components using symmetrical component theory. The impedance profile of the AC network impedance is then easily calculated. For each sequence harmonic component, the corresponding impedance is obtained by taking the ratio of the sequence voltage over the sequence current at that harmonic.

6.1.7 *Optimum Method to Calculate Current and Voltage Harmonic Components*

The DFT method with high sampling frequency should be used to calculate the harmonic components in the measured AC signals. The DFT method is more accurate than the FFT method. This is due to the sampling rates used in the methods. In the FFT method, the sampling rate is set at twice the highest frequency component in the signals. In the DFT method, the sampling rate is set at an extremely high rate. The FFT method is often inaccurate at frequencies around five and a half times the fundamental frequency and at frequencies higher than seven and a half times the fundamental frequency. The DFT method provides accurate calculations at frequencies ranging from 5 Hz to eight times the fundamental frequency. Using the DFT method, accurate impedance profiles are obtained after a short processing delay.

6.1.8 *Impact of HVDC Control System on Impedance Profiling*

The impact of a HVDC control system on impedance profiling was investigated using the International Council on Large Electric Systems (CIGRE) benchmark model. A low interaction between the control system and the modulation signal is desired. Simulation results indicate the HVDC control system does interact with the modulation signal and does affect the impedance measurements. To limit the interaction, the multiple frequency modulation signal should have a limited frequency range.

6.1.9 Impact of AC Network Strength on Impedance Profiling

Accurate profiling of the AC network impedance at a HVDC link was achieved for a variety of network impedance types via the firing angle signal modulation technique. In addition, both strong and weak AC networks were accurately profiled. In general, each frequency component in the modulation signal and the overall modulation signal must be small in magnitude when the AC network is weak. This ensures the firing angle modulation does not affect system operation. On the other hand, each frequency component in the modulation signal must have a large magnitude when the AC network is strong. This guarantees measurable harmonic voltages are generated at the AC bus bar. When the AC network strength is greater than 4 S, it is very difficult to generate such measurable harmonic voltages without disturbing system operation. This is a limitation of the firing angle signal modulation technique. This limitation is not critical, seeing as system behavior is not a large concern when the AC network is especially strong. With a strong AC network the commutating voltage does not vary greatly and there is extremely low risk of commutation failure. In addition, the risk of harmonic instability and resonance is quite low when the AC network is very strong.

6.1.10 Optimum Time to Obtain an AC Network Impedance Profile

Accurate profiling of the AC network impedance at a HVDC link was achieved over a range of system operating points via the firing angle signal modulation technique. The accuracy of the calculated impedance profile improves when the HVDC system operates at a low DC current. This improvement is expected, as the magnitudes of the characteristic harmonic currents injected by the rectifier and inverter into the AC systems generally decrease as the DC current magnitude decreases [8]. The result is an increase in the SNR of the current entering the AC network impedance and a corresponding improvement in the calculated impedance profile. Therefore, the optimum time to modulate the firing angle signal and obtain an AC network impedance profile is while the DC current order is set at a low value.

6.2 Recommendations

The research work completed can be extended in future studies. Rapid identification of the AC network impedance at a HVDC link could be used to optimize system performance. Network resonances could be resolved and impedance dependent operating procedures and protection, damping and control systems could be developed.

Modulation of the control signals of various power electronic devices and flexible AC transmission systems (FACTS) could be investigated. For example, one could modulate the thyristor controlled reactor (TCR) control signal of a static VAr compensator (SVC) in an attempt to measure the impedance at that specific point in the power system. In

addition, the SVC protection, damping and control systems could be made impedance dependent to enhance system reliability, stability and security.

The research models created for this thesis use Power System Computer Aided Design/Electromagnetic Transients Direct Current (PSCAD/EMTDC) software. Future work could be completed to convert these models to equivalent software models on the Real Time Digital Simulator (RTDS), producing simulations in real time.

A physical prototype of an impedance monitor could be built. This hardware device would use the techniques investigated in this thesis to monitor the AC network impedance at a HVDC link via modulation of a HVDC converter firing angle. The prototype could be wire wrapped or a breadboard could be used. The impedance monitor prototype could be tested using RTDS software.

Ultimately, an impedance monitor could be built for use in an operating power system. This would involve card design with solder masked and would be completed after the impedance monitor prototype was tested using RTDS software.

References

[1] X. Jiang, A. M. Gole, "A Frequency Scanning Method for the Identification of Harmonic Instabilities in HVDC Systems," IEEE Transactions on Power Delivery, vol. 10, no. 4, pp. 1875-1881, October, 1995.

[2] I. Papic and A. M. Gole, "Frequency Response Characteristics of the Unified Power Flow Controller," IEEE Transactions on Power Delivery, vol. 18, no. 4, pp. 1394-1402, October, 2003.

[3] M. Mohaddes, A. M. Gole and S. Elez, "Steady State Frequency Response of STATCOM," IEEE Transactions on Power Delivery, vol. 16, no. 1, pp. 18-23, January, 2001.

[4] F.X. Macedo, "Power Harmonic Impedance Measurement Using Natural Disturbances," IEE Special Publication on Sources and Effects of Power System Disturbances, pp. 183-187, 1982.

[5] A.A. Girgis and R.B. McManis, "Frequency Domain Techniques for Modeling Distribution or Transmission Networks Using Capacitor Switching Induced Transients," IEEE Transactions on Power Delivery, vol. 4, no. 3, pp. 1882-1890, July, 1989.

[6] K. Tomiyama, S. Ihara, R.J. Piwko, E.R. Pratico, J.J. Sanchez-Gasca, R.A. Walling and L. Crane, "Impedance Monitor Performance Tests," IEEE Power Engineering Society Winter Meeting, 2002, vol. 1, pp. 538-543, January, 2002.

[7] J. Arrillaga, *High Voltage Direct Current Transmission*. London, England: The Institution of Electrical Engineers, 1998.

[8] A. M. Gole; HVDC Course Notes.

[9] J. D. Ainsworth, "Harmonic instability between controlled static convertors and a.c. networks," IEE Proceedings, vol. 114, no. 7, pp. 949-957, July, 1967.

[10] J. O'Reilly, A. R. Wood and C. M. Osauskas, "Frequency Domain Based Control Design for an HVdc Converter Connected to a Weak AC Network," IEEE Transactions on Power Delivery, vol. 18, no. 3, pp. 1028-1033, July, 2003.

[11] C.L. Phillips and J.M. Parr, *Signals, Systems, and Transforms*. Upper Saddle River, New Jersey, U.S.A.: Prentice-Hall, Inc., 1999.

[12] M. Szechtman et. al., "CIGRE Benchmark Model for DC Controls," Electra, vol. 135, pp. 54-73, April, 1991.

[13] M.S. Roden, *Analog and Digital Communication Systems*. Englewood Cliffs, New Jersey, U.S.A.: Prentice-Hall, Inc., 1979.

[14] P. Kundur, *Power System Stability and Control*. U.S.A.: McGraw-Hill, Inc., 1994.

[15] I.T. Fernando, *Protection of Transmission Lines Sharing the Same Right-of-Way*. Winnipeg, Manitoba, Canada: University of Manitoba, 1997.

[16] A.J. Washington, *Basic Technical Mathematics with Calculus*. Menlo Park, California, U.S.A.: The Benjamin/Cummings Publishing Company, Inc., 1978.

Appendix A: Detailed System Diagrams for Selected Simulation Cases

Case I - Simplified Model of a HVDC Link:

RRLLC Type Impedance,

Multiple Frequency Modulation Signal,

FFT Analysis

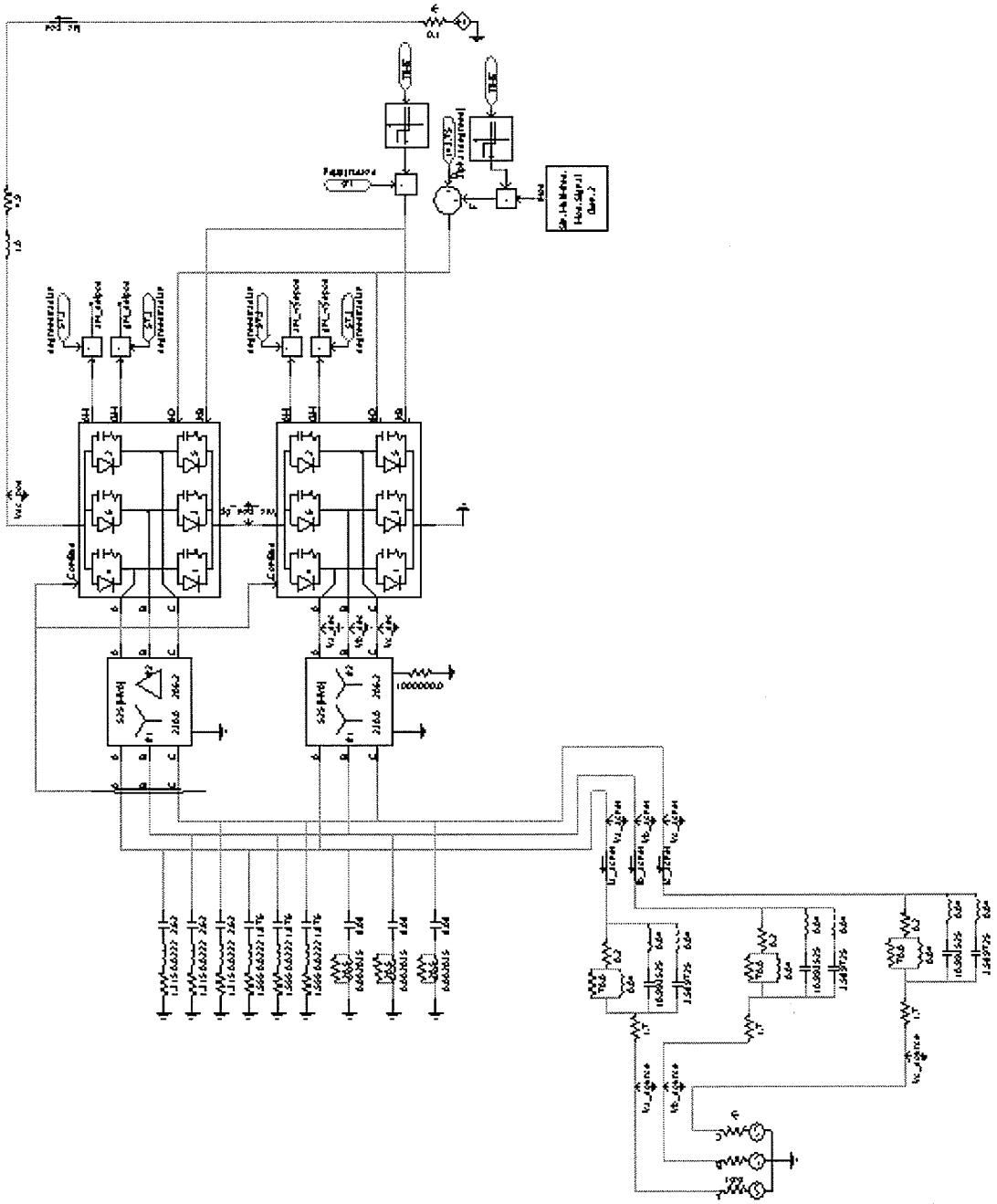

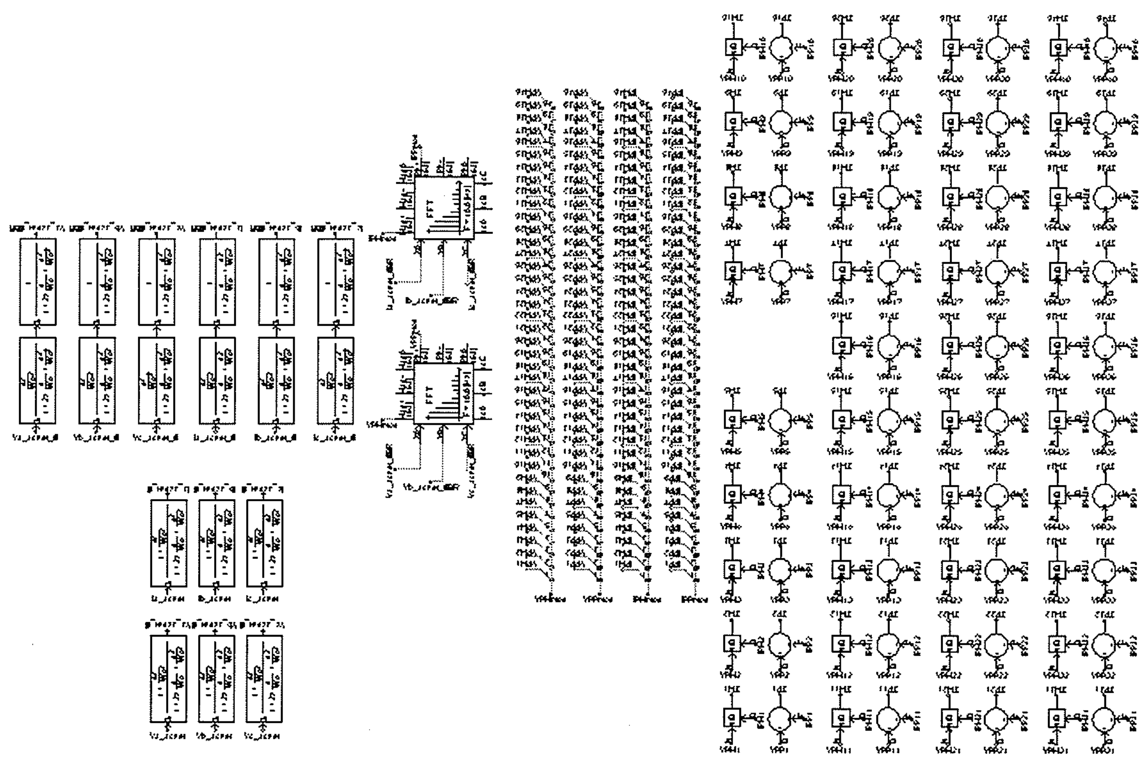

mod
mod10
mod20
mod30
mod40
mod50
mod60
mod70
mod80
mod90
mod100
mod110
mod120
mod130
mod140
mod150
mod160
mod170
mod180
mod190
mod200
mod210
mod220
mod230
mod240
mod250
mod260
mod270
mod280
mod290
mod300
mod310
mod320
mod330
mod340
Sin
phase shift
modulation mag.
0.144
0.09
0.054
0.036
0.019
0.126
0.072

Case II - CIGRE Benchmark Model of a HVDC Link:

Weak Inverter AC Network,

DFT Analysis

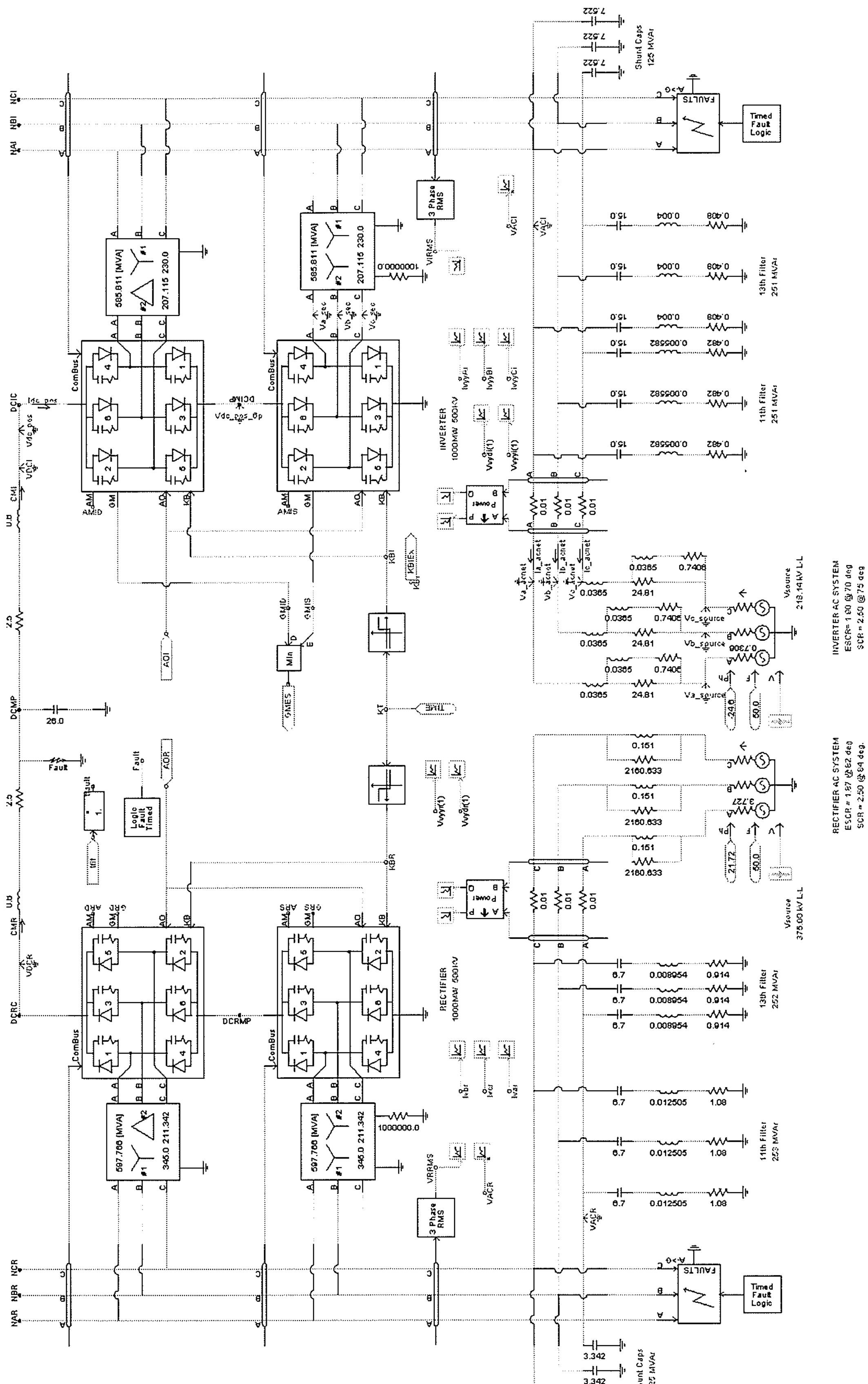

RECTIFIER
1000MW 500kV
INVERTER
1000MW 500kV
RECTIFIER AC SYSTEM
ESCR = 1.87 @ 82 deg
SCR = 2.50 @ 84 deg.
50 Hz@345kV
INVERTER AC SYSTEM
ESCR= 1.00 @ 70 deg
SCR = 2.50 @ 75 deg
50 Hz@230kV
Vsource
375.00 kV L-L
Vsource
218.14kV L-L
11th Filter
251 MVAr
13th Filter
251 MVAr
11th Filter
253 MVAr
13th Filter
252 MVAr
Shunt Caps
125 MVAr
Timed
Fault
Logic
FAULTS
3 Phase
RMS
585.811 [MVA]
207.115 230.0
597.766 [MVA]
345.0 211.342